

Quantum Sensing with Nanoelectronics: Fisher Information for an Adiabatic Perturbation

George Mihailescu, Anthony Kiely, and Andrew K. Mitchell

School of Physics, University College Dublin, Belfield, Dublin 4, Ireland and

Centre for Quantum Engineering, Science, and Technology, University College Dublin, Ireland

Quantum systems used for metrology can offer enhanced precision over their classical counterparts. The design of quantum sensors can be optimized by maximizing the quantum Fisher information (QFI), which characterizes the precision of parameter estimation for an ideal measurement. Here we consider the response of a quantum system as a means to estimate the strength of an external perturbation that has been switched on slowly. General expressions for the QFI are derived, which also hold for interacting many-body systems in the thermodynamic limit at finite temperatures, and can be related to linear-response transport coefficients. For quantum dot nanoelectronics devices, we show that electron interactions can lead to *exponential* scaling of the QFI with system size, highlighting that quantum resources can be utilized in the full Fock space. The precision estimation of voltages and fields can also be achieved by practical global measurements, such as the electric current, making quantum circuits good candidates for metrological applications.

Parameter estimation is a key part of any experiment, both in terms of calibration and readout; and the technological applications of devices for precision sensing are diverse. Scientific discoveries in the modern era have long been driven by our ability to make ever more precise measurements, from the Michelson–Morley interferometer to LIGO [1]. In the context of new quantum technologies such as NISQ devices [2], or other experiments on quantum systems, parameter estimation techniques may themselves be inherently quantum [3, 4]. Indeed, the use of quantum systems as sensors can provide an advantage in terms of precision over classical counterparts [5–8]. Atomic, molecular and optical systems have been widely studied in this regard [5, 9–16].

In this work we explore nanoelectronics devices [17–19] as an alternative and promising platform for quantum sensing. The charge or electrical current through a contacted nanostructure can be accurately measured in an external circuit, and can depend sensitively on voltages, fields, and temperature [20]. Entanglement and quantum many-body effects arising from electron interactions such as Coulomb blockade [21, 22], Kondo effect [17, 23–25] and quantum criticality [26–29] observed in such devices may be a useful resource for sensing. They are also appealing from a practical perspective, since sophisticated quantum devices can now be fabricated in commercial-process semiconductor technologies [30–33].

We consider a general scenario in which the response of a quantum system to an external perturbation is used to estimate the strength of this perturbation. We focus on the case of a perturbation that is switched on slowly. Under the adiabatic approximation we obtain exact expressions for the quantum Fisher information (QFI) [3, 4], which characterizes the maximum precision of parameter estimation attainable by making measurements on the system, see Fig. 1(a). We then apply this to models of quantum dot (QD) nanoelectronics circuits [17], Fig. 1(b), and compare with the estimated precision for

a current measurement in such devices.

Intuitively, the more sensitive the state of a system $\hat{\rho}_\lambda$ is to changes in the external perturbation λ , the more information about the perturbation that can be gained from measurements on the system. For a given number N of independent measurements, the precision of estimation for λ is characterized by its statistical variance $\text{Var}(\lambda) = \mathbb{E}[(\lambda_{\text{est}} - \lambda)^2]$, which for unbiased estimators is controlled by the QFI $F_Q[\lambda]$ through the Cramér-Rao bound (CRB) [34] $N\text{Var}(\lambda) \geq 1/F_Q[\lambda]$. The QFI corresponds to the optimal measurement and is therefore the best-case scenario against which any practical measurement scheme should be compared. The design of advanced quantum sensors therefore necessitates the characterization and optimization of the QFI.

We take an arbitrary system \hat{H}_0 , initially at thermal equilibrium, to which we adiabatically introduce a small perturbation $\lambda\hat{A}$. Our main result is an expression for

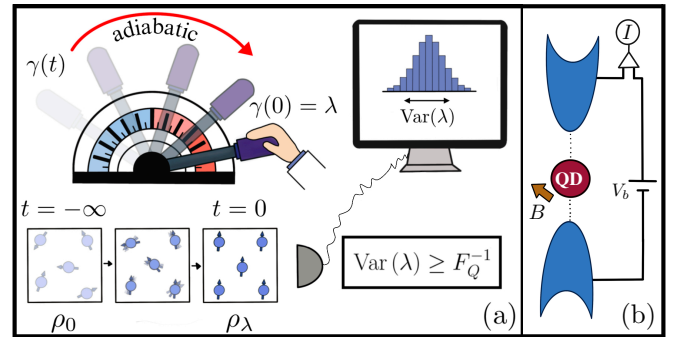


FIG. 1. Adiabatic quantum sensing paradigm. (a) A system is subject to a perturbation λ that was switched on slowly. Measurements of the system response yield statistics on the estimator for λ whose variance is constrained by the QFI Eq. 1 via the CRB. (b) A typical nanoelectronics setup in which an electrical current I flows through a quantum dot due to a bias voltage V_b between source and drain leads in a field B .

the QFI for estimation of the parameter λ ,

$$F_Q[\lambda] = 2 \sum_{n \neq m} \frac{(p_n^0 - p_m^0)^2}{p_n^0 + p_m^0} \frac{|\langle n_0 | \hat{A} | m_0 \rangle|^2}{(E_n^0 - E_m^0)^2}, \quad (1a)$$

$$= -\frac{2}{\pi} \int d\omega \frac{\tanh(\omega/2T)}{\omega^3} \chi(\omega), \quad (1b)$$

where $\hat{H}_0 |n_0\rangle = E_n^0 |n_0\rangle$ and the density matrix $\hat{\rho}_0 = \sum_n p_n^0 |n_0\rangle \langle n_0|$ characterizes the unperturbed state of the system at inverse temperature $\beta \equiv 1/T$, with $p_n^0 = \exp(-\beta E_n^0)/Z_0$ and $Z_0 = \sum_m \exp(-\beta E_m^0)$. Eq. 1a expresses the QFI for a small dc perturbation $\lambda \hat{A}$ in terms of properties of the unperturbed system \hat{H}_0 . The Kubo formula [35] allows us to write this in Eq. 1b in terms of the dynamical linear-response transport coefficient $\chi(\omega) = \frac{d}{d\lambda} \langle \dot{A} \rangle |_{\lambda \rightarrow 0}$, with $\dot{A} = \frac{d}{dt} \hat{A}$ the current induced by a small ac perturbation $\lambda \cos(\omega t) \hat{A}$ [36]. Eq. 1b immediately implies that the *optimal* measurement on a quantum system yields *perfect* metrological sensitivity due to a diverging QFI when the $\omega \rightarrow 0$ dc conductance is finite. *Derivation via adiabatic gauge potential.*— The adiabatic switch-on of the operator \hat{A} can be viewed as a smooth time-dependent perturbation $\hat{H}_1(t) = \gamma(t) \hat{A}$ subject to boundary conditions $\gamma \rightarrow 0$ as $t \rightarrow -\infty$ and $\gamma = \lambda$ at $t = 0$, see Fig. 1(a). We therefore label $\hat{H}_\gamma = \hat{H}_0 + \gamma(t) \hat{A}$ by the running value of γ at time t . The instantaneous spectral decomposition reads $\hat{H}_\gamma = \sum_n E_n^\gamma |n_\gamma\rangle \langle n_\gamma|$. For adiabatic evolution [36], states stay in these instantaneous eigenstates and so

$$\hat{\rho}_\gamma = \sum_n p_n^0 |n_\gamma\rangle \langle n_\gamma| = \hat{U}_\gamma \hat{\rho}_0 \hat{U}_\gamma^\dagger. \quad (2)$$

The second equality follows from the relation,

$$\partial_\gamma |n_\gamma\rangle = i \hat{G}_\gamma |n_\gamma\rangle, \quad (3)$$

where the generator \hat{G}_γ of the adiabatic evolution is known as the adiabatic gauge potential [37, 38]. Since $|n_{\gamma+d\gamma}\rangle = e^{i d\gamma \hat{G}_\gamma} |n_\gamma\rangle$ it follows that $|n_\gamma\rangle \simeq \hat{U}_\gamma |n_0\rangle$ with $\hat{U}_\gamma = e^{i\gamma \hat{G}_0}$ when γ is small. The QFI for estimating λ from a state transformed by Eq. 2 is then [4, 36],

$$F_Q[\lambda] = 2 \sum_{n \neq m} \frac{(p_n^0 - p_m^0)^2}{p_n^0 + p_m^0} |\langle m_0 | \hat{G}_0 | n_0 \rangle|^2 \equiv \text{Var}(\hat{G}_0). \quad (4)$$

To find the relation between \hat{G}_0 and the physical perturbation \hat{A} , we note that $\partial_\gamma \langle m_\gamma | \hat{H}_\gamma | n_\gamma \rangle = i(E_m^\gamma - E_n^\gamma) \langle m_\gamma | \hat{G}_\gamma | n_\gamma \rangle + \langle m_\gamma | \partial_\gamma \hat{H}_\gamma | n_\gamma \rangle$. Since $\partial_\gamma \hat{H}_\gamma = \hat{A}$ and $\langle m_\gamma | \hat{H}_\gamma | n_\gamma \rangle = 0$ for $n \neq m$, we thus find,

$$\langle m_\gamma | \hat{G}_\gamma | n_\gamma \rangle = i \frac{\langle m_\gamma | \hat{A} | n_\gamma \rangle}{E_m^\gamma - E_n^\gamma} \quad : \quad n \neq m \quad (5)$$

which, upon substitution into Eq. 4 yields Eq. 1a. An alternative perturbative derivation is given in the Supplementary Material (SM) [36]. In a different context,

Ref. [39] obtained a similar result but crucially without the excitation energy denominator in Eq. 1a.

Susceptibilities and transport coefficients.— We introduce the retarded real-time correlation function $\bar{K}(t) = -i\theta(t) \langle [\hat{A}(0), \hat{A}(t)] \rangle_0$ evaluated in the unperturbed Hamiltonian \hat{H}_0 , where $\hat{\Omega}(t) = e^{i\hat{H}_0 t} \hat{\Omega} e^{-i\hat{H}_0 t}$. The Lehmann representation of its Fourier transform $\bar{K}(\omega) \equiv \langle \langle \hat{A}; \hat{A} \rangle \rangle = \int dt \exp(i\omega t) \bar{K}(t)$ reads, $\text{Im} \bar{K}(\omega) = \pi \sum_{n,m} (p_n^0 - p_m^0) |\langle n_0 | \hat{A} | m_0 \rangle|^2 \delta(\omega - E_m^0 + E_n^0)$. With the identity $\int d\omega \omega^{-2} \tanh(\omega/2T) \delta(\omega - E_m^0 + E_n^0) = \frac{p_n^0 - p_m^0}{p_n^0 + p_m^0} \times (E_n^0 - E_m^0)^{-2}$ we may express Eq. 1a as,

$$F_Q[\lambda] = \frac{2}{\pi} \int d\omega \frac{\tanh(\omega/2T)}{\omega^2} \text{Im} \bar{K}(\omega), \quad (6)$$

in terms of the susceptibility $\bar{K}(\omega)$, which is a physical observable. This exact expression holds equally well for interacting quantum many-body systems in the thermodynamic limit as well as finite or closed quantum systems.

Since $\text{Im} K(\omega) = \omega^2 \text{Im} \bar{K}(\omega)$ [36], where $K(\omega)$ is the Fourier transform of the current-current correlator $K(t) = -i\theta(t) \langle [\dot{A}(0), \dot{A}(t)] \rangle$, we may further relate the QFI to linear-response (LR) transport coefficients. With an ac bias perturbation $\lambda \cos(\omega t) \hat{A}$ switched on adiabatically, the ac conductance $\chi(\omega) = -\text{Im} K(\omega)/\omega$ follows from the Kubo formula [35, 40]. This gives Eq. 1b.

Nanoelectronic quantum sensors.— We turn now to the application and implications of the above for quantum nanoelectronic devices. We focus on the simplest model for a single semiconductor QD with local Coulomb interaction, coupled to source and drain leads – the celebrated Anderson impurity model (AIM) [17, 41, 42],

$$\hat{H}_0 = \epsilon_d \left(d_\uparrow^\dagger d_\uparrow + d_\downarrow^\dagger d_\downarrow \right) + U_d \left(d_\uparrow^\dagger d_\uparrow d_\downarrow^\dagger d_\downarrow \right) \quad (7)$$

$$+ t \sum_{j=1}^L \sum_{\alpha, \sigma} \left(c_{\alpha j \sigma}^\dagger c_{\alpha j+1 \sigma} + \text{H.c.} \right) + V \sum_{\alpha, \sigma} \left(d_\sigma^\dagger c_{\alpha 1 \sigma} + \text{H.c.} \right)$$

where $\alpha = s, d$ for source and drain leads, $\sigma = \uparrow, \downarrow$ for up and down spin, $c_{\alpha j \sigma}^{(\dagger)}$ are annihilation (creation) operators for the conduction electrons, and $d_\sigma^{(\dagger)}$ are QD operators. Here we have given the Hamiltonian for each of the leads in the form of a 1d nanowire comprising L sites. This allows us to study the scaling of the QFI with system size. The thermodynamic limit, where quantum transport can be meaningfully considered, corresponds to $L \rightarrow \infty$. The noninteracting ($U_d = 0$) limit of this model is the resonant level model (RLM), which can be solved exactly using Green's function methods. For finite L up to around $L = 8$, the interacting AIM can be solved directly using exact diagonalization (ED). The full AIM with $L \rightarrow \infty$ can also be solved with sophisticated many-body techniques such as the numerical renormalization group (NRG) [43]. We combine these methods below to study the metrological capability of the AIM.

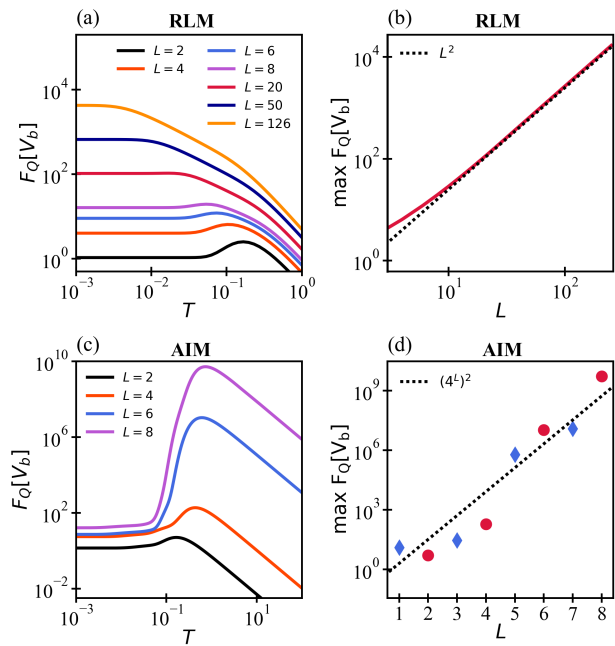


FIG. 2. QFI for an adiabatic voltage bias perturbation in the noninteracting RLM with $U_d = 0$ in (a,b) compared with interacting AIM for $U_d = 0.2$ in (c,d). $F_Q[V_b]$ plotted vs temperature T for finite leads of L sites in (a,c) and the scaling of the maximum QFI with L shown in (b,d). Asymptotes as dotted lines. Parameters: $t = 0.4$, $V = 0.2$ and $\epsilon_d = -U_d/2$.

Voltometry.— We consider first a bias voltage perturbation switched on adiabatically, with $\lambda = -eV_b$ and $\hat{A} = \frac{1}{2}(\hat{N}_s - \hat{N}_d)$, where $\hat{N}_\alpha = \sum_{j=1}^L \hat{n}_{\alpha j}$ is the total number operator for lead α and $\hat{n}_{\alpha j} = \sum_{\sigma} c_{\alpha j \sigma}^\dagger c_{\alpha j \sigma}$. This perturbation can be defined for finite or infinite L . For infinite leads in the quantum transport context, the natural observable is the (average) electrical current into the drain lead, $I \equiv \langle \hat{I} \rangle$ with current operator $\hat{I} = -e\hat{N}_d$. In LR, $I = \chi^{dc} V_b$, where $\chi^{dc} = \lim_{\omega \rightarrow 0} \chi(\omega)$ is the dc conductance. χ^{dc} is naturally finite in any typical nano-electronics setup, and so the QFI $F_Q[V_b]$ for estimating the bias voltage diverges according to Eq. 1b. Fundamentally, this is because the QFI relates to estimating a global parameter using an arbitrarily complex global measurement, in an infinite Fock space.

It is however instructive to examine *how* the QFI diverges with system size L . As shown in the SM [36], the adiabatic voltage QFI for the AIM can be cast exactly as

$$F_Q[V_b] = 4V^2 \sum_{k,p} \frac{\tanh\left(\frac{\xi_k - \epsilon_p}{2T}\right)}{(\xi_k - \epsilon_p)^4} [f(\epsilon_p) - f(\xi_k)] a_k b_p, \quad (8)$$

where a_k and ξ_k are the trivial pole weights and energies of the free (disconnected) lead density of states $\rho_0(\omega) = \sum_{k=1}^L a_k \delta(\omega - \xi_k)$ whereas b_p and ϵ_p the pole weights and energies of the full lead-coupled QD spectral function $A_{QD}(\omega) = \sum_p b_p \delta(\omega - \epsilon_p)$. $f(\omega)$ is the Fermi function.

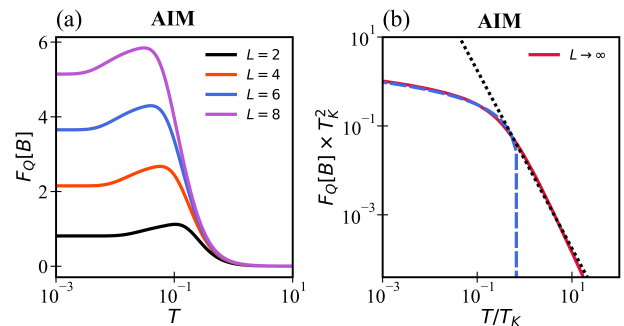


FIG. 3. QFI for a local magnetic field B applied adiabatically in the AIM. (a) ED results for $F_Q[B]$ vs T in systems with finite leads using the same parameters as Fig. 2c. (b) NRG results for the AIM in the thermodynamic limit of infinite leads, scaled in terms of the Kondo temperature T_K , for $U_d = 0.2$, $\epsilon_d = -0.1$, $V = 0.07$, $t = 0.5$ in the universal regime. Dotted/dashed lines are the asymptotes discussed in the text.

For the noninteracting RLM, the sum on p runs over all $2L + 1$ poles of the full system, \hat{H}_0 . In this case ϵ_p are the single-particle energies in the diagonal representation $\hat{H}_0 = \sum_{p\sigma} \epsilon_p f_{p\sigma}^\dagger f_{p\sigma}$ and b_p is the weight of eigenstate p on the QD orbital. Fig. 2(a) shows the resulting QFI for representative model parameters as a function of temperature T for different system sizes. As anticipated we see a saturation of $F_Q[V_b]$ for $T \ll t/L$ due to the existence of a minimum excitation gap $|\xi_k - \epsilon_p|$ in the finite system, and we generally see better sensitivity at lower temperatures. Fig. 2(b) shows Heisenberg-type scaling of the QFI with the system size [44–48], $\max F_Q[V_b] \sim L^2$. The low- T QFI increases as the excitation gap closes. Because the system is noninteracting, the quantum resources being utilized here are essentially the single-particle states.

For the interacting AIM, Figs. 2(c,d), the story is quite different. The Lehmann representation of the QD spectral function $A_{QD}(\omega)$ now involves exponentially-many terms, corresponding to the proliferation of many-particle excitations [49]. We now see very strong, roughly exponential scaling, $\max F_Q[V_b] \sim (4^L)^2$ consistent with the growth of the underlying Fock space with L . This highlights that optimal global measurements may exploit the full Fock space in strongly correlated systems [36].

Magnetometry.— We now consider a local magnetic field perturbation $\lambda \hat{A} = B \hat{S}_d^z$ in the AIM (the RLM has no spin dynamics since $\sigma = \uparrow, \downarrow$ are decoupled for $U_d = 0$). The magnetometry QFI is computed from Eq. 6 using the QD dynamical spin susceptibility $\bar{K}(\omega) = \langle\langle \hat{S}_d^z; \hat{S}_d^z \rangle\rangle$ [50], obtained for small finite systems via ED in Fig. 3(a) and via NRG [49] for $L \rightarrow \infty$ in Fig. 3(b).

The ED results for $F_Q[B]$ vs T with finite leads show only a modest increase of sensitivity with L . Even though the underlying Fock space dimension increases exponentially with L , information on the local perturbation is seemingly not strongly imprinted on all many-particle

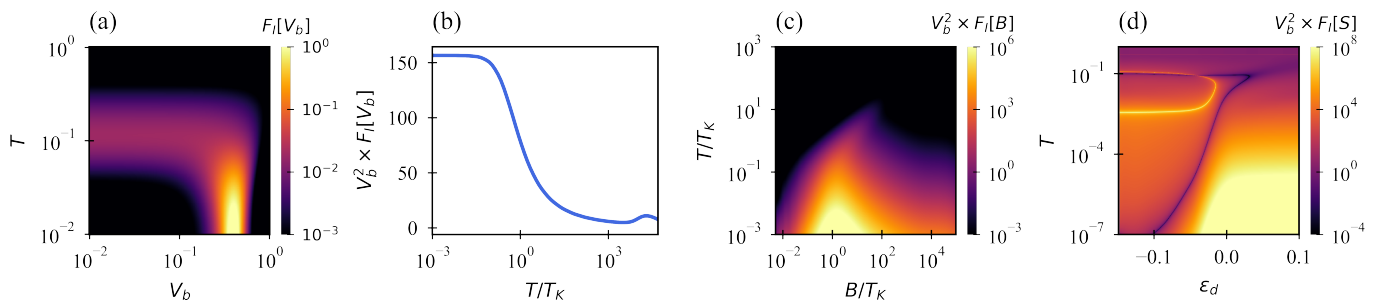


FIG. 4. Quantum metrology with current measurements. (a) Precision of voltage estimation $F_I[V_b]$ in the nonequilibrium RLM as a function of V_b and T for $\epsilon_d = -0.2$, $\Gamma = 0.05$. (b,c,d) NRG results for interacting AIM with $U_d = 0.3$, $\Gamma = 0.013$ in linear response. (b) $F_I[V_b]$ vs T/T_K in the universal Kondo regime for $\epsilon_d = -0.15$. (c) Magnetometry $F_I[B]$ vs T/T_K and B/T_K with $\epsilon_d = -0.15$. (d) $F_I[S]$ vs T and ϵ_d for estimation of the QD entropy S from a current measurement. See [36] for details.

states (unlike for the extensive voltage perturbation). Jumping to the case with infinite leads in Fig. 3(b), we in fact find a finite $F_Q[B]$ for all finite T . To understand this behavior of the QFI one must understand the physics of the AIM and its spin dynamics. At half-filling, the interacting QD hosts a spin- $\frac{1}{2}$ local moment, which becomes dynamically screened by conduction electrons at low temperatures $T \ll T_K$ due to the formation of a many-body singlet state through a process known as the Kondo effect [41]. The Kondo temperature T_K is an emergent low-energy scale in terms of which physical properties exhibit universal scaling [43]. While an asymptotically-free local moment is polarized by an infinitesimal field, giving a diverging dynamical spin susceptibility, the QD local moment in the AIM only starts to become polarized for $B \sim T_K$ due to formation of the Kondo singlet [51]. On the lowest energy scales, $\bar{K}(\omega) \sim \omega$ [50] and thus Eq. 6 is finite. Up to log corrections, our NRG results are consistent with the ansatz $\text{Im}\bar{K}(\omega) \sim \frac{\omega/T_K^2}{1+(T/T_K)^2+(\omega/T_K)^2}$ in the universal regime $|\omega|, T \ll U_d$, from which we extract the universal asymptotes $T_K^2 F_Q[B] \sim (T_K/T)^2$ for $T \gg T_K$ (Fig. 3(b), dotted line) and $\sim \log[T_K/T]$ for $T \ll T_K$ (dashed line), in agreement with NRG data. Our results are also consistent with Eq. 1b since the field cannot induce a persistent dc spin current, and so $\chi(0) = 0$.

Estimation from current measurement. – While the QFI considered above provides a bound on the best possible sensitivity, the optimal global measurement in a many-body system is typically impractical. For nanoelectronics devices, the standard experimental measurement [17] is the electrical current I due to a bias voltage V_b switched on adiabatically (but λ can be a parameter of \hat{H}_0). The error-propagation formula [4] gives the precision $F_I[\lambda]$ for estimating parameter λ from a current measurement,

$$F_I[\lambda] \equiv 1/\text{Var}(\lambda) = |\partial_\lambda \langle \hat{I} \rangle|^2 / \text{Var}(I), \quad (9)$$

and $F_Q[\lambda] \geq F_I[\lambda]$. The precision is equal to the classical Fisher information when current measurements are Gaussian distributed [52].

For the noninteracting RLM the current is given by the Landauer-Büttiker (LB) formula [40, 53], $\langle \hat{I} \rangle = \frac{e}{h} \int d\omega \mathcal{T}(\omega) \times [f(\omega - \mu_s) - f(\omega - \mu_d)]$ which holds even at finite bias $eV_b = \mu_s - \mu_d$, with μ_α the chemical potential of lead α . We assume for simplicity a flat lead density of states $\rho_0(\omega) = \rho_0 \Theta(D - |\omega|)$ in a band of halfwidth $D \equiv 1$, and hybridization $\Gamma = \pi \rho_0 V^2$. For the RLM the transmission function is then given by $\mathcal{T}(\omega) = 4\pi \Gamma A_{QD}(\omega)$ in terms of the QD spectral function, which takes a Lorentzian form [36]. We consider instantaneous current measurements and so $\text{Var}(I) = \frac{1}{2\pi} \int d\omega S(\omega)$ in terms of the nonequilibrium noise spectrum $S(\omega)$ [36], which can similarly be obtained in closed form from the transmission function via the Lesovik formula [36, 54]. In Fig. 4(a) we use this machinery to compute $F_I[V_b]$ for voltage estimation. We see that resonances in the QD transmission function enhance the precision at sweet-spot values of T and V_b . Unlike the QFI, the precision $F_I[V_b]$ is finite, despite the current being a global measurement.

For the interacting AIM the situation is more subtle, since the LB and Lesovik formulae no longer apply [55]. We therefore restrict to LR and use NRG to compute the current from the Kubo formula [35, 36, 40] $\chi^{dc} = \lim_{\omega \rightarrow 0} \text{Im}K(\omega)/\omega$ for $\hat{A} = \frac{1}{2}[\hat{N}_s - \hat{N}_d]$ as before. $\text{Var}(I)$ is again obtained from the noise spectrum, which in LR follows from the fluctuation-dissipation relation $S(\omega) = n_B(\omega) \text{Im}K(\omega)/\pi$ with $n_B(\omega)$ the Bose-Einstein distribution [36]. Fig. 4(b) shows $F_I[V_b]$ vs T/T_K for the AIM, indicating a dramatic enhancement to precision at low temperatures due to the Kondo effect. In panel (c) we consider instead magnetometry in the AIM, showing a nontrivial precision profile, with strongly enhanced performance at low $T \ll T_K$ for fields $B \sim T_K$.

Finally, we briefly examine the capability of estimating thermodynamic properties using current measurements. Recent interest in measuring the entropy S of a QD system [56–58] motivates us to compute the precision $F_I[S]$ in Fig. 4(d). We do this from Eq. 9 by rewriting $\partial_S \langle \hat{I} \rangle = \partial_{\epsilon_d} \langle \hat{I} \rangle / \partial_{\epsilon_d} S$ and then exploiting the Maxwell

relation $\partial_{\epsilon_d} S = -\partial_T \langle \hat{n}_d \rangle$ in terms of the QD charge $\hat{n}_d = \sum_{\sigma} d_{\sigma}^{\dagger} d_{\sigma}$. The required derivatives are obtained from NRG results for the evolution of $\langle \hat{I} \rangle$ and $\langle \hat{n}_d \rangle$ with T and ϵ_d . Fig. 4(d) shows highly nontrivial behavior, with distinct regions of the precision phase diagram corresponding to the different renormalization group fixed points of the AIM [41]. Further details in the SM include the case of an integrated current measurement [36].

Conclusion.— The metrological performance of a quantum system can be optimized by maximizing its QFI and measurement-specific precision. Here we developed a general strategy for computing the QFI for an adiabatic perturbation to a quantum many-body system and applied it to models of nanoelectronics devices. For generic extensive perturbations we expect the QFI for the optimal global measurement to grow exponentially in the number of degrees of freedom for strongly correlated systems, since the full Fock space can in principle be utilized. The effective single-particle states in noninteracting systems appear to be a much weaker quantum resource for metrology. Local perturbations will typically yield a finite QFI even in the thermodynamic limit. These features are illustrated for voltometry and magnetometry in the AIM describing semiconductor QD devices.

The precision for practical measurements may be far from the QFI ideal – even for global measurements, as with the electrical current in QD devices. This presents ample opportunity to optimize the design and measurement protocol for nanoelectronics devices beyond the single QD paradigm. Many-body quantum effects [17, 59] and quantum criticality [28, 29] engineered in such systems may provide a route to enhanced sensing [60–63].

The adiabatic gauge potential [64, 65] has recently been computed using the Lanczos algorithm and might provide a route to the QFI beyond linear response. Our results have potential impact beyond metrology, since the QFI plays many roles in different areas of quantum science and technology e.g. witness for entanglement [66], measure of non-Markovianity [67, 68], resource quantifier in quantum thermodynamics [69] and fidelity susceptibility in quantum control [70], quantum speed limits [71], optimisation of variational quantum algorithms [72], and for continuous measurement currents [73–77].

Acknowledgments.— We thank Steve Campbell, Mark Mitchison, Abolfazl Bayat, Tomohiro Shitara and Adeline Crépieux for insightful discussions. We acknowledge financial support from Science Foundation Ireland through Grant 21/RP-2TF/10019 (AKM) and Equal1 Laboratories Ireland Limited (GM).

[1] D. V. Martynov, E. Hall, B. Abbott, R. Abbott, T. Abbott, C. Adams, R. Adhikari, R. Anderson, S. Anderson, K. Arai, *et al.*, Phys. Rev. D **93**, 112004 (2016).

[2] J. Preskill, Quantum **2**, 79 (2018).
 [3] M. G. A. Paris, Int. J. Quantum Inf. **07**, 125 (2009).
 [4] G. Tóth and I. Apellaniz, J. Phys. A: Math. Theor **47**, 424006 (2014).
 [5] C. L. Degen, F. Reinhard, and P. Cappellaro, Rev. Mod. Phys. **89**, 035002 (2017).
 [6] V. Giovannetti, S. Lloyd, and L. Maccone, Nature Photonics **5**, 222 (2011).
 [7] J. Yang, S. Pang, A. del Campo, and A. N. Jordan, Phys. Rev. Res. **4**, 013133 (2022).
 [8] N. Aslam, H. Zhou, E. K. Urbach, M. J. Turner, R. L. Walsworth, M. D. Lukin, and H. Park, Nat. Rev. Phys. **5**, 157 (2023).
 [9] J. Ye and P. Zoller, Phys. Rev. Lett. **132**, 190001 (2024).
 [10] J. C. Pelayo, K. Gietka, and T. Busch, Phys. Rev. A **107**, 033318 (2023).
 [11] K. Gietka and H. Ritsch, Phys. Rev. Lett. **130**, 090802 (2023).
 [12] R. Di Candia, F. Minganti, K. Petrovnin, G. Paraoanu, and S. Felicetti, npj Quantum Information **9**, 23 (2023).
 [13] Z.-J. Ying, S. Felicetti, G. Liu, and D. Braak, Entropy **24**, 1015 (2022).
 [14] V. Montenegro, G. S. Jones, S. Bose, and A. Bayat, Phys. Rev. Lett. **129**, 120503 (2022).
 [15] F. Troiani and M. G. A. Paris, Phys. Rev. Lett. **120**, 260503 (2018).
 [16] F. Albarelli, M. Rossi, M. Paris, and M. Genoni, New J. Phys. **19**, 123011 (2017).
 [17] D. Goldhaber-Gordon, H. Shtrikman, D. Mahalu, D. Abusch-Magder, U. Meirav, and M. A. Kastner, Nature **391**, 156 (1998); W. Van der Wiel, S. D. Franceschi, T. Fujisawa, J. Elzerman, S. Tarucha, and L. Kouwenhoven, Science **289**, 2105 (2000).
 [18] M. L. Perrin, E. Burzuri, and H. S. J. van der Zant, Chem. Soc. Rev. **44**, 902 (2015); Z. Chen, I. M. Grace, S. L. Woltering, L. Chen, A. Gee, J. Baugh, G. A. D. Briggs, L. Bogani, J. A. Mol, C. J. Lambert, H. L. Anderson, and J. O. Thomas, Nat. Nanotechnol. , 1 (2024).
 [19] K. Nowack, F. H. L. Koppens, Y. V. Nazarov, and L. M. K. Vandersypen, Science **318**, 1430 (2007); P. Barthelemy and L. M. K. Vandersypen, Annalen der Physik **525**, 808 (2013).
 [20] T. Ihn, *Semiconductor Nanostructures: Quantum states and electronic transport* (OUP Oxford, 2009).
 [21] U. Meirav, M. A. Kastner, and S. J. Wind, Phys. Rev. Lett. **65**, 771 (1990).
 [22] J. Park, A. Pasupathy, J. Goldsmith, C. Chang, Y. Yaish, J. Petta, M. Rinkoski, J. Sethna, H. Abruña, P. McEuen, and D. Ralph, Nature **417**, 722 (2002).
 [23] W. Liang, M. Shores, M. Bockrath, J. Long, and H. Park, Nature **417**, 725 (2002).
 [24] A. Keller, S. Amasha, I. Weymann, C. Moca, I. Rau, J. Katine, D. Shtrikman, G. Zaránd, and D. Goldhaber-Gordon, Nat.Phys. **10**, 145 (2014).
 [25] C. Piquard, P. Glidic, C. Han, A. Aassime, A. Cavanna, U. Gennser, Y. Meir, E. Sela, A. Anthore, and F. Pierre, Nat. Commun. **14**, 7263 (2023).
 [26] R. Potok, I. Rau, H. Shtrikman, Y. Oreg, and D. Goldhaber-Gordon, Nature **446**, 167 (2007).
 [27] N. Roch, S. Florens, B. Bouchiat, W. Wernsdorfer, and F. Balestro, Nature **453**, 633 (2008).
 [28] Z. Iftikhar, A. Anthore, A. K. Mitchell, F. D. Parmentier, U. Gennser, A. Ouerghi, A. Cavanna, C. Mora, P. Simon, and F. Pierre, Science **360**, 1315 (2018).

- [29] W. Pouse, L. Peeters, C. L. Hsueh, U. Gennser, A. Cavanna, M. A. Kastner, A. K. Mitchell, and D. Goldhaber-Gordon, *Nat. Phys.* **19**, 492 (2023); D. B. Karki, E. Boulat, W. Pouse, D. Goldhaber-Gordon, A. K. Mitchell, and C. Mora, *Phys. Rev. Lett.* **130**, 146201 (2023).
- [30] E. Chanrion, D. J. Niegemann, B. Bertrand, C. Spence, B. Jadot, J. Li, P. Mortemousque, L. Hutin, R. Maurand, X. Jehl, M. Sanquer, S. De Franceschi, C. Bäuerle, F. Balestro, Y. Niquet, M. Vinet, T. Meunier, and M. Urdampilleta, *Phys. Rev. Appl.* **14**, 024066 (2020).
- [31] X. Xue, B. Patra, J. P. G. van Dijk, N. Samkharadze, S. Subramanian, A. Corna, B. Paquelet Wuetz, C. Jeon, F. Sheikh, E. Juarez-Hernandez, B. Esparza, H. Ramapurawala, B. Carlton, S. Ravikumar, C. Nieva, S. Kim, H. Lee, A. Sammak, G. Scappucci, M. Veldhorst, F. Sebastiano, M. Babaie, S. Pellerano, E. Charbon, and L. M. K. Vandersypen, *Nature* **593**, 205 (2021).
- [32] A. Ruffino, T. Yang, J. Michniewicz, Y. Peng, E. Charbon, and M. Gonzalez-Zalba, *Nature Electronics* **5**, 53 (2022).
- [33] N. Petropoulos, X. Wu, A. Sokolov, P. Giounanlis, I. Bashir, A. K. Mitchell, M. Asker, D. Leipold, R. B. Staszewski, and E. Blokhina, *Appl. Phys. Lett.* **124**, 173503 (2024).
- [34] S. L. Braunstein and C. M. Caves, *Phys. Rev. Lett.* **72**, 3439 (1994).
- [35] R. Kubo, *J. Phys. Soc. Jpn.* **12**, 570 (1957).
- [36] “Supplementary Material.”
- [37] M. Berry, *J. Phys. A: Math. Theor.* **42**, 365303 (2009).
- [38] M. Kolodrubetz, D. Sels, P. Mehta, and A. Polkovnikov, *Phys. Rep.* **697**, 1 (2017).
- [39] P. Hauke, M. Heyl, L. Tagliacozzo, and P. Zoller, *Nat. Phys.* **12**, 778 (2016).
- [40] E. Minarelli, J. Rigo, and A. Mitchell, (2022), arXiv:2209.01208.
- [41] A. Hewson, *The Kondo problem to heavy fermions* (Cambridge Studies in Magnetism, CUP, 1993).
- [42] M. Pustilnik and L. Glazman, *J. Phys. Condens. Matter* **16**, R513 (2004).
- [43] R. Bulla, T. A. Costi, and T. Pruschke, *Rev. Mod. Phys.* **80**, 395 (2008).
- [44] K. Gietka, F. Metz, T. Keller, and J. Li, *Quantum* **5**, 489 (2021).
- [45] R. Demkowicz-Dobrzański, J. Kołodyński, and M. Guță, *Nat. Commun.* **3**, 1063 (2012).
- [46] M. Zwierz, C. A. Pérez-Delgado, and P. Kok, *Phys. Rev. A* **85**, 042112 (2012).
- [47] M. Zwierz, C. A. Pérez-Delgado, and P. Kok, *Phys. Rev. Lett.* **105**, 180402 (2010).
- [48] M. M. Rams, P. Sierant, O. Dutta, P. Horodecki, and J. Zakrzewski, *Phys. Rev. X* **8**, 021022 (2018).
- [49] A. Weichselbaum and J. von Delft, *Phys. Rev. Lett.* **99**, 076402 (2007).
- [50] M. Hanl and A. Weichselbaum, *Phys. Rev. B* **89**, 075130 (2014).
- [51] T. A. Costi, *Phys. Rev. Lett.* **85**, 1504 (2000).
- [52] D. Ding, Z. Liu, B. Shi, G. Guo, K. Mølmer, and C. Adams, *Nat. Phys.* **18**, 1447 (2022).
- [53] M. Büttiker, Y. Imry, R. Landauer, and S. Pinhas, *Phys. Rev. B* **31**, 6207 (1985).
- [54] G. B. Lesovik, *JETP Letters* **49**, 513 (1989).
- [55] Y. Meir and N. S. Wingreen, *Phys. Rev. Lett.* **68**, 2512 (1992).
- [56] N. Hartman, C. Olsen, S. Lüscher, M. Samani, S. Fallahi, G. Gardner, M. Manfra, and J. Folk, *Nat. Phys.* **14**, 1083 (2018).
- [57] C. Han, Z. Iftikhar, Y. Kleeorin, A. Anthore, F. Pierre, Y. Meir, A. K. Mitchell, and E. Sela, *Phys. Rev. Lett.* **128**, 146803 (2022).
- [58] T. Child, O. Sheekey, S. Lüscher, S. Fallahi, G. C. Gardner, M. Manfra, A. K. Mitchell, E. Sela, Y. Kleeorin, Y. Meir, and J. Folk, *Phys. Rev. Lett.* **129**, 227702 (2022).
- [59] A. K. Mitchell, K. G. L. Pedersen, P. Hedegård, and J. Paaske, *Nat. Commun.* **8**, 15210 (2017); S. Sen and A. Mitchell, (2023), arXiv:2310.14775.
- [60] I. Frérot and T. Roscilde, *Phys. Rev. Lett.* **121**, 020402 (2018).
- [61] G. Mihailescu, S. Campbell, and A. K. Mitchell, *Phys. Rev. A* **107**, 042614 (2023).
- [62] G. Mihailescu, A. Bayat, S. Campbell, and A. Mitchell, *Quantum Sci. Technol.* **9**, 035033 (2024).
- [63] G. Di Fresco, B. Spagnolo, D. Valenti, and A. Carollo, *SciPost Phys.* **13**, 077 (2022).
- [64] K. Takahashi and A. del Campo, *Phys. Rev. X* **14**, 011032 (2024).
- [65] S. Morawetz and A. Polkovnikov, (2024), arXiv:2401.12287.
- [66] P. Laurell, A. Scheie, E. Dagotto, and D. Tennant, (2024), arXiv:2405.10899.
- [67] J. Liu, H. Yuan, X. Lu, and X. Wang, *J. Phys. A: Math. Theor.* **53**, 023001 (2019).
- [68] S. Scandi, P. Abiuso, J. Surace, and D. De Santis, (2024), arXiv:2304.14984.
- [69] I. Marvian, *Phys. Rev. Lett.* **129**, 190502 (2022).
- [70] P. M. Poggi, G. De Chiara, S. Campbell, and A. Kiely, *Phys. Rev. Lett.* **132**, 193801 (2024).
- [71] S. Deffner and S. Campbell, *J. Phys. A: Math. Theor.* **50**, 453001 (2017).
- [72] J. J. Meyer, *Quantum* **5**, 539 (2021).
- [73] S. Gammelmark and K. Mølmer, *Phys. Rev. A* **87**, 032115 (2013).
- [74] S. Gammelmark and K. Mølmer, *Phys. Rev. Lett.* **112**, 170401 (2014).
- [75] M. Radaelli, J. A. Smiga, G. T. Landi, and F. C. Binder, (2024), arXiv:2402.06556.
- [76] T. Ilias, D. Yang, S. Huelga, and M. Plenio, *PRX Quantum* **3**, 010354 (2022).
- [77] J. Boeyens, B. Annby-Andersson, G. Bakhshinezhad, P. and Haack, M. Perarnau-Llobet, P. Nimmrichter, S. and Potts, and M. Mehboudi, *New J. Phys.* **25**, 123009 (2023).

SUPPLEMENTARY MATERIAL
Quantum Sensing with Nanoelectronics:
Fisher Information for an Adiabatic Perturbation

George Mihailescu, Anthony Kiely, and Andrew K. Mitchell
School of Physics, University College Dublin, Belfield, Dublin 4, Ireland and
Centre for Quantum Engineering, Science, and Technology, University College Dublin, Ireland

S-I. QFI UNDER ADIABATIC EVOLUTION

We consider in this work an arbitrary Hamiltonian \hat{H}_0 , to which we apply a small (dc) perturbation $\hat{H}_1 = \gamma \hat{A}$ that is switched on adiabatically in the infinitely distant past. We examine the response of the system to the perturbation at time $t = 0$ as a means to estimate the perturbation strength. In particular, we wish to calculate the quantum Fisher information (QFI) for the perturbation after the adiabatic evolution of the system.

We take our quantum system to be initially in thermal equilibrium, described by the thermal density matrix $\hat{\rho}_0 = \exp(-\beta \hat{H}_0)/Z_0$ at inverse temperature β , where $Z_0 = \text{Tr}[\exp(-\beta \hat{H}_0)]$ is the partition function of \hat{H}_0 . We set $k_B \equiv 1$ and $\hbar \equiv 1$. In the energy eigenbasis we have $\hat{H}_0|n_0\rangle = E_n^0|n_0\rangle$ and $\hat{\rho}_0 = \sum_n p_n^0|n_0\rangle\langle n_0|$, where $p_n^0 = \exp(-\beta E_n^0)/Z_0$ are the probabilities. The full Hamiltonian, including the perturbation, reads,

$$\hat{H}_\gamma = \hat{H}_0 + \gamma \hat{A}. \quad (\text{S-1})$$

The adiabatic switch-on of the perturbation is encoded through the time-dependence $\gamma(t)$. For concreteness, suppose that $\gamma(t) = \lambda \times e^{-|t|}$, which describes the adiabatic transformation from \hat{H}_0 at time $t = -\infty$ to $\hat{H}_\lambda = \hat{H}_0 + \lambda \hat{A}$ at $t = 0$. The instantaneous spectral decomposition reads $\hat{H}_\gamma = \sum_n E_n^\gamma|n_\gamma\rangle\langle n_\gamma|$ and the density matrix is $\hat{\rho}_\gamma = \sum_n p_n^\gamma|n_\gamma\rangle\langle n_\gamma|$. However, under adiabatic evolution the states stay in their instantaneous eigenstates and so $p_n^\gamma = p_n^0$ and $|n_\gamma\rangle = \hat{U}_\gamma|n_0\rangle$. From this it follows that the density matrix at $t = 0$ for a system with an adiabatic perturbation is given by,

$$\hat{\rho}_\lambda = \sum_n p_n^0|n_\lambda\rangle\langle n_\lambda| = \hat{U}_\lambda \hat{\rho}_0 \hat{U}_\lambda^\dagger. \quad (\text{S-2})$$

The general expression for the QFI for a parameter λ imprinted on a density matrix $\hat{\rho}_\lambda$ is given by,¹

$$F_Q[\lambda] = \sum_n \frac{(\partial_\lambda p_n^\lambda)^2}{p_n^\lambda} + 2 \sum_{n \neq m} \frac{(p_n^\lambda - p_m^\lambda)^2}{p_n^\lambda + p_m^\lambda} |\langle m_\lambda | \partial_\lambda n_\lambda \rangle|^2, \quad (\text{S-3})$$

which for Eq. S-2 reduces to,

$$F_Q[\lambda] = 2 \sum_{n \neq m} \frac{(p_n^0 - p_m^0)^2}{p_n^0 + p_m^0} |\langle m_0 | \hat{U}_\lambda^\dagger (\partial_\lambda \hat{U}_\lambda) | n_0 \rangle|^2, \quad (\text{S-4})$$

where the first term of Eq. S-3 vanishes because the probabilities p_n^0 are those of the unperturbed Hamiltonian \hat{H}_0 . If we now suppose a general form for the unitary $\hat{U}_\lambda = e^{i\lambda \hat{\mathcal{O}}}$ then we can write $\langle m_0 | \hat{U}_\lambda^\dagger (\partial_\lambda \hat{U}_\lambda) | n_0 \rangle = \langle m_0 | e^{-i\lambda \hat{\mathcal{O}}} (i\hat{\mathcal{O}}) e^{i\lambda \hat{\mathcal{O}}} | n_0 \rangle = i \langle m_0 | \hat{\mathcal{O}} | n_0 \rangle$ and hence,

$$F_Q[\lambda] = 2 \sum_{n \neq m} \frac{(p_n^0 - p_m^0)^2}{p_n^0 + p_m^0} |\langle m_0 | \hat{\mathcal{O}} | n_0 \rangle|^2 \equiv \text{Var}(\hat{\mathcal{O}}). \quad (\text{S-5})$$

This holds for any perturbation λ provided that it is switched on adiabatically.

A. Perturbation Theory

For a small perturbation λ , we can obtain the states of \hat{H}_λ perturbatively to first order in λ ,

$$\begin{aligned} |n_\lambda\rangle &\approx |n_0\rangle + \lambda \sum_{m \neq n} \frac{\langle m_0 | \hat{A} | n_0 \rangle}{E_n^0 - E_m^0} |m_0\rangle \\ &= |n_0\rangle - i\lambda \hat{W} |n_0\rangle \end{aligned} \quad (\text{S-6})$$

where the correction to the wavefunction normalization can be neglected to leading order, and where

$$\hat{W} = \sum_{j \neq m} \frac{i \langle m_0 | \hat{A} | j_0 \rangle}{E_j^0 - E_m^0} |m_0\rangle \langle j_0| \quad (\text{S-7})$$

is an Hermitian operator. Inserting this into our expression for $\hat{\rho}_\lambda$ in Eq. S-2 we obtain

$$\begin{aligned} \hat{\rho}_\lambda &\approx \sum_n p_n^0 \left(|n_0\rangle - i\lambda \hat{W} |n_0\rangle \right) \left(\langle n_0| + i\lambda \langle n_0| \hat{W}^\dagger \right) \\ &\approx \hat{\rho}_0 - i\lambda [\hat{W}, \hat{\rho}_0] \end{aligned} \quad (\text{S-8})$$

where we have truncated to linear order in the perturbation λ in the second line.

Finally, we note that when λ is a small parameter, the BCH expansion of Eq. S-2 with $\hat{U}_\lambda = e^{i\lambda \hat{O}}$ may be truncated at leading commutator order, which yields,

$$\hat{\rho}_\lambda \simeq \hat{\rho}_0 - i\lambda [\hat{O}, \hat{\rho}_0] \quad (\text{S-9})$$

Comparing Eqs. S-8 and S-9 we can identify the operator \hat{O} with \hat{W} . This analysis shows that a small perturbation switched on adiabatically can be understood as a phase-imprinting unitary rotation of the unperturbed thermal state of the system. The QFI $F_Q[\lambda]$ for estimation of the perturbation λ must be calculated with respect to the operator \hat{W} . Substituting our result Eq. S-7 into Eq. S-5 with $\hat{O} = \hat{W}$ we obtain,

$$F_Q[\lambda] = 2 \sum_{n \neq m} \frac{(p_n^0 - p_m^0)^2}{p_n^0 + p_m^0} \frac{|\langle n_0 | \hat{A} | m_0 \rangle|^2}{(E_n^0 - E_m^0)^2}. \quad (\text{S-10})$$

As shown in the main text, this result can also be obtained using the concept of the adiabatic gauge potential. This may provide a route to generalizing our present results beyond the perturbative regime.

B. QFI from susceptibilities

Our Eq. S-10 can be cast in the alternative form of a susceptibility, similar to the famous result of Ref. 2, by using the identity,

$$\int d\omega \frac{\tanh(\omega/2T)}{\omega^2} \delta(\omega - E_m^0 + E_n^0) = \frac{p_n^0 - p_m^0}{p_n^0 + p_m^0} \times \frac{1}{(E_n^0 - E_m^0)^2}. \quad (\text{S-11})$$

Together with the the definition of the correlation function,

$$\text{Im} \bar{K}(\omega) = \pi \sum_{n,m} (p_n^0 - p_m^0) |\langle n_0 | \hat{A} | m_0 \rangle|^2 \delta(\omega - E_m^0 + E_n^0), \quad (\text{S-12})$$

we can now express the QFI as

$$F_Q[\lambda] = \frac{2}{\pi} \int d\omega \frac{\tanh(\omega/2T)}{\omega^2} \text{Im} \bar{K}(\omega). \quad (\text{S-13})$$

Here, $\bar{K}(\omega) \equiv \langle \langle \hat{A}; \hat{A} \rangle \rangle = \int dt \exp(i\omega t) \bar{K}(t)$ is the Fourier transform of the retarded, real-time correlator $\bar{K}(t) = -i\theta(t) \langle [\hat{A}(0), \hat{A}(t)] \rangle_0$, where $\hat{\Omega}(t) = e^{i\hat{H}_0 t} \hat{\Omega} e^{-i\hat{H}_0 t}$. $\bar{K}(\omega)$ is evaluated in \hat{H}_0 and its Lehmann representation is given by Eq. S-12. Thus, the QFI for an adiabatic perturbation is a physical observable, since the susceptibility is a physical observable and experimentally measurable in principle.

We note the difference between Eq. S-13 and the result in Ref. 2, which expresses Eq. S-5 in terms of the susceptibility for the operator \hat{O} , without connecting it to any physical perturbation. By recognizing that the generator of the evolution for the quantum state model $\hat{\rho}_\lambda = \hat{U}_\lambda \hat{\rho}_0 \hat{U}_\lambda^\dagger$ is \hat{W} in Eq. S-7 and not the perturbation \hat{A} itself, we get an additional squared excitation energy denominator in the expression for the QFI. This has important consequences. However, it does not affect the results or conclusions of Ref. 2, which were obtained in a different context and did not address quantum parameter estimation.

It may be convenient to express Eq. S-13 in terms of a related correlation function. We now introduce the retarded current-current correlation function $K(\omega) \equiv \langle\langle \dot{A}; \dot{A} \rangle\rangle$, where $\dot{A} = \frac{d}{dt}\hat{A}$. Here $K(\omega)$ is the Fourier transform of $K(t) = -i\theta(t)\langle[\dot{A}(0), \dot{A}(t)]\rangle_0$, again evaluated in \hat{H}_0 . Using bosonic Green's function equations of motion,³

$$\omega\langle\langle \hat{X}; \hat{Y} \rangle\rangle - \langle[\hat{X}, \hat{Y}]\rangle = \langle\langle \hat{X}; [\hat{H}, \hat{Y}] \rangle\rangle = \langle\langle [\hat{X}, \hat{H}]; \hat{Y} \rangle\rangle$$

with $\hat{\Omega} \equiv \frac{d}{dt}\hat{\Omega} = i[\hat{H}, \hat{\Omega}]$, we find that $\langle\langle \dot{A}; \dot{A} \rangle\rangle = \omega^2\langle\langle \hat{A}; \hat{A} \rangle\rangle + \omega\langle[\hat{A}, [\hat{A}, \hat{H}_0]]\rangle$. Since \hat{A} and \hat{H}_0 are both Hermitian, $\langle[\hat{A}, [\hat{A}, \hat{H}_0]]\rangle$ is real, and therefore $\text{Im}K(\omega) = \omega^2\text{Im}\bar{K}(\omega)$. Thus we can write,

$$F_Q[\lambda] = \frac{2}{\pi} \int d\omega \frac{\tanh(\omega/2T)}{\omega^4} \text{Im}K(\omega), \quad (\text{S-14})$$

which expresses the QFI for a perturbation λ in terms of the correlation function for the associated currents \dot{A} .

C. QFI from transport coefficients

As shown above, the QFI for an adiabatic perturbation can be computed from correlation functions evaluated in the unperturbed system at equilibrium. The linear response of a system to a weak perturbation can also be expressed in terms of equilibrium correlation functions via the Kubo formula. As we show below, it is possible to relate the QFI for an adiabatic perturbation to dynamical linear response transport coefficients – even though the perturbation for which we compute the QFI is dc steady-state.

Generalizing to an ac perturbation, we define,

$$\hat{H}'_1(t) = \lambda \cos(\omega t) \hat{A}, \quad (\text{S-15})$$

where ω is the ac frequency. Taking the perturbation λ to be small, we can look at the response of the system to the perturbation in terms of the induced currents that flow, to linear order in λ . Within linear response, it follows that,

$$\langle \dot{A} \rangle = \chi(\omega) \lambda \quad (\text{S-16})$$

where $\chi(\omega) = \frac{d}{d\lambda} \langle \dot{A} \rangle|_{\lambda \rightarrow 0}$ is the ac-frequency-dependent linear-response transport coefficient, and $\dot{A} = \frac{d}{dt} \hat{A}$.

The Kubo formula^{4,5} allows us to calculate the transport coefficient in terms of *equilibrium* properties of the unperturbed system \hat{H}_0 ,

$$\chi(\omega) = -\frac{\text{Im}K(\omega)}{\omega} \quad (\text{S-17})$$

where $K(\omega) \equiv \langle\langle \dot{A}; \dot{A} \rangle\rangle$ as before. We have set $\hbar \equiv 1$. Equivalently, this may be expressed in terms of $\bar{K}(\omega)$ in Eq. S-12,

$$\chi(\omega) = -\omega \text{Im}\bar{K}(\omega). \quad (\text{S-18})$$

The dc limit corresponds to taking $\omega \rightarrow 0$, such that $\hat{H}_1(t) \rightarrow \hat{H}_1 = \lambda \hat{A}$ and $\chi(\omega) \rightarrow \chi_{\text{dc}}$ where,

$$\chi_{\text{dc}} = -\lim_{\omega \rightarrow 0} [\omega \text{Im}\bar{K}(\omega)] = -\lim_{\omega \rightarrow 0} [\text{Im}K(\omega)/\omega]. \quad (\text{S-19})$$

When the dc transport coefficient χ_{dc} is finite, the low-frequency behaviour of the correlation functions is therefore $\text{Im}\bar{K}(\omega) \sim 1/\omega$ and $\text{Im}K(\omega) \sim \omega$.

It is now clear that the QFI for a small adiabatic dc perturbation λ can be understood in terms of the ac linear-response transport coefficient $\chi(\omega)$ corresponding to the currents $\langle \dot{A} \rangle$ induced by the operator \hat{A} coupling to λ ,

$$F_Q[\lambda] = -\frac{2}{\pi} \int d\omega \frac{\tanh(\omega/2T)}{\omega^3} \chi(\omega) \quad (\text{S-20})$$

An immediate consequence is that $F_Q[\lambda]$ is divergent (infinite) unless $\chi(\omega)$ vanishes faster than ω .

S-II. QFI FOR THE ANDERSON IMPURITY MODEL

A nontrivial application is to quantum dot (QD) nanoelectronics devices. Here we define \hat{H}_0 as the QD nanostructure coupled to source and drain leads at equilibrium. The leads are held at the same chemical potential and have the same temperature; everything is at zero field. In general, the QD-leads coupling can be strong,⁶ and electronic interactions cannot typically be neglected because quantum confinement in any nano-scale device ubiquitously results in Coulomb blockade physics.⁷ The ensuing macroscopic entanglement between the QD and leads at low temperatures can produce highly non-markovian dynamics, such as the Kondo effect.⁸

We model our equilibrium nanodevice as a generalized quantum impurity model⁹ of the form $\hat{H}_0 = \hat{H}_{\text{leads}} + \hat{H}_{\text{nano}} + \hat{H}_{\text{hyb}}$. In the quantum transport setup, the nanostructure is tunnel-coupled to infinite source and drain leads, which are taken to be continuum reservoirs of non-interacting conduction electrons, in the thermodynamic limit.

The approach we develop can be straightforwardly generalized to more complex nanostructures but for the sake of a simple demonstration, we restrict ourselves here to a single QD orbital, tunnel-coupled symmetrically to source and drain leads. With local Coulomb interactions on the QD, this is the celebrated Anderson impurity model (AIM):⁸

$$\hat{H}_0 = t \sum_{j=1}^L \sum_{\alpha,\sigma} \left(c_{\alpha j \sigma}^\dagger c_{\alpha j+1 \sigma} + \text{H.c.} \right) + \epsilon_d \sum_{\sigma} \left(d_{\sigma}^\dagger d_{\sigma} \right) + U_d \left(d_{\uparrow}^\dagger d_{\uparrow} d_{\downarrow}^\dagger d_{\downarrow} \right) + V \sum_{\alpha,\sigma} \left(d_{\sigma}^\dagger c_{\alpha 1 \sigma} + \text{H.c.} \right), \quad (\text{S-21})$$

where $\alpha = s, d$ for source and drain leads, $\sigma = \uparrow, \downarrow$ for up and down spin, $c_{\alpha j \sigma}^{(\dagger)}$ are annihilation (creation) operators for the conduction electrons, and $d_{\sigma}^{(\dagger)}$ are annihilation (creation) operators for the QD. Here we have given the Hamiltonian for the each of the leads in the form of a 1d nanowire, comprising L sites. This allows us to study the scaling of the QFI with system size. The thermodynamic limit corresponds to $L \rightarrow \infty$. The noninteracting ($U_d = 0$) limit of this model is the resonant level model (RLM).

One useful simplification arising in the case of the AIM or RLM is the ‘proportionate coupling’ QD-lead hybridization geometry.¹⁰ This means that we may introduce even and odd lead orbital combinations: $c_{ej\sigma} = \frac{1}{\sqrt{2}}(c_{sj\sigma} + c_{dj\sigma})$ and $c_{oj\sigma} = \frac{1}{\sqrt{2}}(c_{sj\sigma} - c_{dj\sigma})$. The QD then only couples to the even lead orbitals in \hat{H}_0 and the odd lead orbitals formally decouple. The Hamiltonian for the leads takes exactly the same form as in Eq. S-21 but now $\alpha = e, o$. The hybridization part of the Hamiltonian becomes simply $H_{\text{hyb}} = \sqrt{2}V \sum_{\sigma} (d_{\sigma}^\dagger c_{e1\sigma} + \text{H.c.})$. This effective one-channel description is not essential to the following, but does permit an elegant description.

To this model we add a perturbation \hat{H}_1 , switched on adiabatically, and study the resulting QFI for this perturbation. In the following we consider, separately, a voltage bias perturbation and a magnetic field applied to the QD.

A. Bias Voltage Perturbation

First we consider applying an ac bias voltage,

$$\hat{H}_1(t) = -eV_b \cos(\omega t) \frac{1}{2} \left[\hat{N}_s - \hat{N}_d \right], \quad (\text{S-22})$$

where V_b is the bias voltage, taken to be split equally across source and drain leads. Here $\hat{N}_\alpha = \sum_{j\sigma} c_{\alpha j \sigma}^\dagger c_{\alpha j \sigma}$ is the total number operator for lead α . This perturbation can be defined for the model with finite or infinite L .

In this setup $\lambda = -eV_b$ and $\hat{A} = \frac{1}{2}(\hat{N}_s - \hat{N}_d)$. For infinite leads in the quantum transport context, the natural observable is the (average) electrical current into the drain lead, $\langle \hat{I} \rangle$ with current operator $\hat{I} = -e\dot{N}_d$ and $\dot{N}_\alpha = \frac{d}{dt} \hat{N}_\alpha$. For infinite leads, due to current conservation we have $\langle \dot{N}_s \rangle = -\langle \dot{N}_d \rangle$. In linear response we may write $\langle \hat{I} \rangle = \chi(\omega)V_b$ with $\chi(\omega)$ the ac conductance. The dc conductance is simply $\chi^{dc} = \chi(\omega \rightarrow 0)$, and is typically finite. The conductance is given in units of e^2/h . From the Kubo formula,^{4,5} $\chi(\omega) = \left(\frac{e^2}{h} \right) \times \frac{2\pi\omega}{4} \text{Im} \langle \langle \hat{N}_s - \hat{N}_d; \dot{N}_s - \dot{N}_d \rangle \rangle$, which is evaluated at equilibrium in \hat{H}_0 . The QFI for estimation of the bias voltage in the dc limit is therefore,

$$F_Q[V_b] = \frac{2}{\pi} \int d\omega \frac{\tanh(\omega/2T)}{\omega^3} \chi(\omega), \quad (\text{S-23})$$

where here and in the following we set $\hbar \equiv 1$, $e \equiv 1$ and $k_B \equiv 1$.

With infinite leads as thermal reservoirs, χ^{dc} is typically finite and so the integral is divergent, meaning an infinite voltage QFI. However, an interesting question addressed in the following is *how* the QFI diverges with system size? For finite L it is no longer meaningful to talk of quantum transport and steady state currents. Therefore we express the voltage QFI directly via Eq. S-14 in terms of the correlation function $K(\omega)$.

1. Green's function formulation

For the following discussion, it will be useful to find an efficient formulation for the QFI in terms of the QD retarded Green's function. The key object is the correlator $K(\omega) = \frac{1}{4} \langle \langle \dot{N}_s - \dot{N}_d; \dot{N}_s - \dot{N}_d \rangle \rangle$, where $\dot{N}_\alpha = \sum_{j=1}^L \sum_\sigma c_{\alpha j \sigma}^\dagger c_{\alpha j \sigma}$ and $\dot{N}_\alpha = \frac{d}{dt} \hat{N}_\alpha = i[\hat{H}, \hat{N}_\alpha]$. Thus we find,

$$K(\omega) = -\frac{1}{2} V^2 \sum_{\sigma, \sigma'} \langle \langle (d_{\sigma'}^\dagger c_{o1\sigma} - \text{H.c.}); (d_{\sigma'}^\dagger c_{o1\sigma'} - \text{H.c.}) \rangle \rangle = \frac{1}{2} V^2 \sum_{\sigma} \left[\langle \langle d_{\sigma}^\dagger c_{o1\sigma}; c_{o1\sigma}^\dagger d_{\sigma} \rangle \rangle + \langle \langle c_{o1\sigma}^\dagger d_{\sigma}; d_{\sigma}^\dagger c_{o1\sigma} \rangle \rangle \right], \quad (\text{S-24})$$

where the second equality follows from the fact that the odd conduction electron sector is decoupled and is therefore subject to separate charge and spin conservation. Furthermore, the retarded correlators can be decomposed into independent contributions corresponding to the decoupled even and odd sectors. After some manipulations we obtain,

$$\text{Im } K(\omega) = \pi V^2 \int d\omega' A_{QD}(\omega') \times [\rho_0(\omega' - \omega) \{f_{\text{eq}}(\omega' - \omega) - f_{\text{eq}}(\omega')\} - \rho_0(\omega' + \omega) \{f_{\text{eq}}(\omega' + \omega) - f_{\text{eq}}(\omega')\}], \quad (\text{S-25})$$

where $A_{QD}(\omega) = -\frac{1}{\pi} \text{Im } G_{QD}(\omega)$ is the QD spectral function, and where $G_{QD}(\omega) \equiv \langle \langle d_{\sigma}; d_{\sigma}^\dagger \rangle \rangle$ is the full lead-coupled QD retarded Green's function, evaluated in \hat{H}_0 (which is independent of spin σ). Also, we have used $\rho_0(\omega) = -\frac{1}{\pi} \text{Im } \mathcal{G}_{\text{lead}}(\omega)$ as the density of states of the free, uncoupled, leads at the QD position. It is given in terms of the free leads Green's function $\mathcal{G}_{\text{lead}}(\omega) \equiv \langle \langle c_{\alpha 1 \sigma}; c_{\alpha 1 \sigma}^\dagger \rangle \rangle_0$, which is taken to be independent of channel α and spin σ . As we see later, it is crucial in certain circumstances to keep track of the finite lead bandwidth, and so here we retain the full lead density of states as an arbitrary function for generality. The equilibrium Fermi-Dirac distribution is denoted $f_{\text{eq}}(\omega) = [e^{\omega/T} + 1]^{-1}$. We note that Eq. S-25 is exact, holds for interacting or noninteracting models, and for finite lead length L as well as in the thermodynamic limit $L \rightarrow \infty$.

With a knowledge of the lead density of states $\rho_0(\omega)$ and the QD spectral function $A_{QD}(\omega)$ we can evaluate $K(\omega)$ and hence the voltage QFI,

$$F_Q[V_b] = 4V^2 \int d\omega \int d\omega' \frac{\tanh(\frac{\omega - \omega'}{2T})}{(\omega - \omega')^4} [f_{\text{eq}}(\omega') - f_{\text{eq}}(\omega)] \times \rho_0(\omega) A_{QD}(\omega'). \quad (\text{S-26})$$

For $L \rightarrow \infty$ we have $t\mathcal{G}_{\text{lead}}(\omega) = \omega/2t - i\sqrt{1 - (\omega/2t)^2}$ such that $\rho_0(\omega) = \frac{1}{\pi t} \sqrt{1 - (\omega/2t)^2} \Theta(1 - |\omega/2t|)$ is finite within a band of halfwidth $D = 2t$. For the noninteracting RLM, the lead-coupled QD Green's function reads,

$$G_{QD}^{RLM}(\omega) = \frac{1}{\omega - \epsilon_d - 2V^2 \mathcal{G}_{\text{lead}}(\omega)}. \quad (\text{S-27})$$

$A_{QD}(\omega)$ is then approximately Lorentzian, with a peak centered on $\omega \sim \epsilon_d$ of width $\sim V^2/t$. Combining these results, we indeed find that the dc electrical conductance $\chi_c^{dc} = \lim_{\omega \rightarrow 0} \text{Im} K(\omega)/\omega$ is finite, and hence the voltage QFI $F_Q[V_b]$ from Eq. S-20 or Eq. S-26 diverges.

For the interacting AIM, the Green's function has a non-trivial self-energy correction,

$$G_{QD}^{AIM}(\omega) = \frac{1}{\omega - \epsilon_d - 2V^2 \mathcal{G}_{\text{lead}}(\omega) - \Sigma(\omega)}, \quad (\text{S-28})$$

but the dc conductance is again finite, and the QFI again diverges.

For finite L , both the free lead density of states $\rho_0(\omega)$ and the lead-coupled QD Green's function $G_{QD}(\omega)$ consist of a finite sum of poles, and the QFI integrals collapse to sums over pole contributions. For the free lead,

$$\rho_0(\omega) = \sum_{k=1}^L a_k \delta(\omega - \xi_k), \quad (\text{S-29})$$

which has L poles for a nanowire lead of length L . In the diagonal basis of lead α , we can write $\hat{H}_{\text{lead}}^\alpha = \sum_{k\sigma} \xi_k c_{\alpha k \sigma}^\dagger c_{\alpha k \sigma}$ and a_k is the weight of free lead state k at the site $j = 1$ coupled to the QD.

On the other hand, for the non-interacting RLM, we can write,

$$A_{QD}(\omega) = \sum_p b_p \delta(\omega - \epsilon_p) \quad (\text{S-30})$$

where the sum over p runs over all $2L + 1$ poles of the full lead-QD-lead composite system. In the diagonal representation of the full (equilibrium) Hamiltonian, $\hat{H}_0 = \sum_{p\sigma} \epsilon_p f_{p\sigma}^\dagger f_{p\sigma}$ with single-particle energies ϵ_p . Here b_p is the weight of eigenstate p on the QD orbital.

In the case of the interacting AIM with finite L , we may still write $A_{QD}(\omega)$ as a sum of poles as per Eq. S-30 but the pole weights and positions must be obtained from the Lehmann representation in the many-particle basis.¹¹ The sum over p includes exponentially-many terms, corresponding to the proliferation of many-particle excitations.

For the finite-sized RLM or AIM, we therefore find that the QFI can be expressed as,

$$F_Q[V_b] = 4V^2 \sum_{k,p} \frac{\tanh\left(\frac{\xi_k - \epsilon_p}{2T}\right)}{(\xi_k - \epsilon_p)^4} [f_{\text{eq}}(\epsilon_p) - f_{\text{eq}}(\xi_k)] \times a_k b_p. \quad (\text{S-31})$$

In general this expression for the QFI yields a finite result, although clearly $F_Q[V_b]$ blows up as the energy gap between single-particle excitation poles closes.

Our numerical results for the noninteracting RLM obtained by diagonalizing the single-particle Hamiltonian \hat{H}_0 shown in Fig. 2(a,b) of the main text demonstrate a scaling $\max(F_Q[V_b]) \sim L^2$. This is the result of entanglement of all $2L + 1$ sites in the system in this setup. However, note that we are ultimately dealing with the single-particle physics of independent electrons: for $2L + 1$ sites in our full system, we have $2L + 1$ poles of the single-particle QD Green's function on which the QFI depends. The energy gap between excitations is then typically $\sim 1/L$.

For the interacting AIM we obtain the QD Green's function of the coupled system using exact diagonalization (ED) in the many-particle basis (exploiting charge and spin symmetries), which we can comfortably do with a basic code up to $L = 8$. We find very strong scaling with system size – roughly exponential, $\max(F_Q[V_b]) \sim (4^L)^2$ – see Fig. 2(c,d).

B. Magnetic Field Perturbation

We now consider adding instead a perturbation to \hat{H}_0 corresponding to a magnetic field B on the QD,

$$\hat{H}_1 = B \hat{S}_d^z, \quad (\text{S-32})$$

with B a Zeeman field along z and $\hat{S}_d^z = \frac{1}{2}[d_\uparrow^\dagger d_\uparrow - d_\downarrow^\dagger d_\downarrow]$ the spin projection of the QD orbital. Due to SU(2) spin symmetry the direction of B is arbitrary. In this case the QFI for estimation of the field strength B is,

$$F_Q[B] = \frac{2}{\pi} \int d\omega \frac{\tanh(\omega/2T)}{\omega^2} \text{Im} \bar{K}(\omega), \quad (\text{S-33})$$

where $\bar{K}(\omega) = \langle\langle S_d^z; S_d^z \rangle\rangle$ is the dynamical spin susceptibility evaluated in \hat{H}_0 . In a Fermi liquid phase⁸ we typically have $\text{Im} \bar{K}(\omega) \sim \omega$. Thus the integral is convergent and $F_Q[B]$ is expected to be finite. Since the perturbation is *local*, the correlation function $\bar{K}(\omega)$ also involves local operators. However, it does of course still encode correlations in the full systems that affect the QD.

The RLM has no spin dynamics since $\sigma = \uparrow$ and $\sigma = \downarrow$ sectors are decoupled. Therefore in the case of magnetometry we must consider the interacting AIM. In Fig. 3 of the main text we compare ED calculations for finite-size systems with numerical renormalization group (NRG) results^{9,11} for the system in the thermodynamic limit. Although we see a modest increase in $F_Q[B]$ with L from ED up to $L = 8$, the QFI does not diverge with L . NRG results for $L \rightarrow \infty$ show a finite magnetometry QFI for any finite T , although the QFI does diverge logarithmically as the temperature T is decreased.

To understand the numerical results for the QFI we note that NRG results for $\text{Im} \bar{K}(\omega)$ are consistent with the ansatz

$$T_K \text{Im} \bar{K}(\omega) \sim \frac{\omega/T_K}{1 + (T/T_K)^2 + (\omega/T_K)^2}, \quad (\text{S-34})$$

where T_K is the Kondo temperature, defined here as the $T = 0$ peak in $\text{Im} \bar{K}(\omega)$. The universal scaling result is approximate but found to be rather accurate for all ω and T considered, up to log corrections. Using our ansatz in Eq. S-33 for the QFI yields directly the scaling prediction that $T_K^2 F_Q[B]$ is a universal scaling function of T/T_K , as confirmed by the full NRG results in Fig. 3(b). Furthermore, we extract from the ansatz the QFI asymptotes $T_K^2 F_Q[B] \sim (T_K/T)^2$ for $T \gg T_K$ and $\sim \log[T_K/T]$ for $T \ll T_K$. We expect similar low- T results for magnetometry in any Fermi liquid, since by the Korrington-Shiba relation⁸ $\text{Im} \bar{K}(\omega) \sim \omega$ for such a system on the lowest energy scales.

S-III. FISHER INFORMATION FOR A CURRENT MEASUREMENT

In the nanoelectronics context, the natural experimental observable is of course the electrical current between source and drain leads passing through the QD. We imagine switching on a bias voltage V_b adiabatically and measuring the current, to estimate some parameter λ . Note that λ here can be a parameter of \hat{H}_0 or \hat{H}_1 , or indeed temperature T , and need not be small. To make contact with the QFI results of the previous sections, here we consider explicitly once again voltometry or magnetometry (estimation of V_b or B), but this time we use the current specifically, rather than the optimal measurement. We focus here on an instantaneous current measurement $\langle \hat{I} \rangle$, although we consider the integrated current (collected charge) in the next section. To characterize the precision of our system to estimation of V_b or B , we use the error-propagation formula to define the quantity,¹

$$F_I[\lambda] = \frac{(\partial_\lambda \langle \hat{I} \rangle)^2}{\text{Var}(I)}, \quad (\text{S-35})$$

where $\text{Var}(I) = \langle \delta \hat{I}^2 \rangle$ and $\delta \hat{I} = \hat{I} - \langle \hat{I} \rangle$ in terms of the current operator $\hat{I} = -e\dot{N}_d$ as before. In general, $F_I[\lambda] \leq \mathcal{F}_I[\lambda]$, where $\mathcal{F}_I[\lambda]$ is the true (classical) Fisher information (FI) for a current measurement. The precision $F_I[\lambda]$ is equal to the FI $\mathcal{F}_I[\lambda]$ when measurement outcomes are Gaussian distributed.¹² Thus we have a chain of inequalities, $F_Q[\lambda] \geq \mathcal{F}_I[\lambda] \geq F_I[\lambda]$, and from the CRB $\text{Var}(\lambda) \geq 1/F_Q[\lambda]$ (one-shot case).¹

The variance of the instantaneous current $\text{Var}(I)$ appearing in Eq. S-35 can be obtained from the current autocorrelator $S(t) = \langle \delta \hat{I}(0) \delta \hat{I}(t) \rangle$ since $S(t=0) = \langle \delta \hat{I}^2 \rangle$. Therefore, $\text{Var}(I)$ can also be calculated by integrating the noise spectrum $S(\omega) = \int dt e^{i\omega t} S(t)$, viz:

$$\text{Var}(I) = S(t=0) = \frac{1}{2\pi} \int d\omega S(\omega). \quad (\text{S-36})$$

We conclude that if we know the current and its noise spectrum, we can calculate the precision for an instantaneous current measurement. In the following we therefore focus on finding expressions for $\langle \hat{I} \rangle$ and $S(\omega)$ for our nanoelectronics models of interest. Note that the electrical current has units e/h , the conductance is in units e^2/h , and the noise has units e^2/h^2 . Unless otherwise stated, we take $e \equiv 1$, $k_B \equiv 1$ and $\hbar \equiv 1$.

For parameter estimation of V_b or B we therefore have,

$$F_I[V_b] = \frac{(G^{dc})^2}{S(t=0)} \quad ; \quad F_I[B] = \frac{(\partial_B \langle \hat{I} \rangle)^2}{S(t=0)} \quad (\text{S-37})$$

where $G^{dc} = d\langle \hat{I} \rangle / dV_b$ is the dc differential conductance, which can be evaluated at any V_b .

A. Linear Response but interacting

In linear response we can apply a small ac bias voltage V_b according to Eq. S-22. The (average) current $\langle \hat{I} \rangle$ is then proportional to the voltage V_b . The proportionality factor is the linear response ac conductance $\chi(\omega)$. For $\omega \rightarrow 0$ this becomes the dc linear response conductance χ^{dc} , which is the differential conductance G^{dc} appearing in Eq. S-37 evaluated in the zero-bias limit $V_b \rightarrow 0$ and we have $\langle \hat{I} \rangle = \chi^{dc} V_b$. In the general ac transport setup, with ω the ac bias frequency, the Kubo formula gives an expression^{4,5} for the linear response conductance $\chi(\omega) = \text{Im} \langle \langle \hat{I}; \hat{I} \rangle \rangle / \omega$. Importantly, the current-current correlation function is evaluated at equilibrium in \hat{H}_0 . Since in \hat{H}_0 at zero bias no net current flows, $\langle \hat{I} \rangle_0 = 0$ and so $\delta \hat{I} \equiv \hat{I} - \langle \hat{I} \rangle = \hat{I}$ at equilibrium. Thus,

$$\chi(\omega) = \text{Im} \langle \langle \delta \hat{I}; \delta \hat{I} \rangle \rangle / \omega \quad ; \quad \lim_{V_b \rightarrow 0} G^{dc} \equiv \chi^{dc} = \lim_{\omega \rightarrow 0} \chi(\omega) \quad (\text{S-38})$$

Furthermore, the fluctuation-dissipation relation tells us that the retarded and lesser Green's functions in equilibrium are connected. Therefore we can write,

$$\pi S(\omega) = n_B(\omega) \text{Im} \langle \langle \delta \hat{I}; \delta \hat{I} \rangle \rangle \equiv \omega n_B(\omega) \chi(\omega), \quad (\text{S-39})$$

where $n_B(\omega) = [e^{\omega/T} - 1]^{-1}$ is the Bose-Einstein distribution. For $F_I(\lambda)$ we need $S(t=0)$, which we can obtain from the ac linear response conductance $\chi(\omega)$, or the current-current correlation function $\langle \langle \delta \hat{I}; \delta \hat{I} \rangle \rangle$.

The above formulation is restricted to linear response, but is otherwise completely general: it makes no assumptions about the form of the nanostructure, which can be single or multi-orbital in any geometry, interacting or non-interacting, and connected to the leads in any geometry. The central object needed is the current-current correlation function evaluation at equilibrium, which can be calculated even for complex interacting systems by e.g. NRG.^{9,11}

1. Single QD case

If we specialize now to the single-QD case of the interacting AIM (or non-interacting RLM) then we can in fact make further simplifications. Up to factors of the electric charge e , \hbar and k_B (which we have set to unity), the current-current correlator $\langle\langle\delta\hat{I};\delta\hat{I}\rangle\rangle = K(\omega)$ is simply the correlator given in Eq. S-25. The dc conductance in linear response for the AIM (or RLM) can then be obtained by inserting Eq. S-25 into Eq. S-38. After some manipulations we recover the famous Meir-Wingreen formula,¹⁰

$$\chi^{dc} = \lim_{\omega \rightarrow 0} [\text{Im } K(\omega)/\omega] = 2\pi V^2 \int d\omega [-\partial_\omega f_{\text{eq}}(\omega)] \rho_0(\omega) A_{QD}(\omega) \quad (\text{S-40})$$

Similarly, inserting Eq. S-25 into Eq. S-39 yields an explicit expression for the equilibrium noise spectrum,

$$\begin{aligned} S(\omega) &= V^2 \int d\omega' A_{QD}(\omega') \times n_B(\omega) [\rho_0(\omega' - \omega) \{f_{\text{eq}}(\omega' - \omega) - f_{\text{eq}}(\omega')\} - \rho_0(\omega' + \omega) \{f_{\text{eq}}(\omega' + \omega) - f_{\text{eq}}(\omega')\}] , \\ &\equiv V^2 \int d\omega' A_{QD}(\omega') \times \left[\rho_0(\omega' - \omega) f_{\text{eq}}(\omega') (1 - f_{\text{eq}}(\omega' - \omega)) + \rho_0(\omega' + \omega) f_{\text{eq}}(\omega' + \omega) (1 - f_{\text{eq}}(\omega')) \right] \end{aligned} \quad (\text{S-41})$$

This can be integrated to find the variance of the instantaneous current,

$$\begin{aligned} \text{Var}(I) &= \int d\omega S(\omega) = \frac{1}{\pi} \int d\omega n_B(\omega) \text{Im } K(\omega) \\ &= V^2 \int \int d\omega d\omega' n_B(\omega) A_{QD}(\omega') \times [\rho_0(\omega' - \omega) \{f_{\text{eq}}(\omega' - \omega) - f_{\text{eq}}(\omega')\} - \rho_0(\omega' + \omega) \{f_{\text{eq}}(\omega' + \omega) - f_{\text{eq}}(\omega')\}] \\ &= \frac{1}{2} V^2 \left[\int d\omega' A_{QD}(\omega') \times \int d\omega \rho_0(\omega) - \int d\omega' \tanh(\omega'/2T) A_{QD}(\omega') \times \int d\omega \tanh(\omega'/2T) \rho_0(\omega) \right] \end{aligned} \quad (\text{S-42})$$

Due to spectral normalization, and for the standard case of a particle-hole symmetric free lead density of states $\rho_0(\omega) = \rho_0(-\omega)$, we therefore have the remarkably simple result,

$$\text{Var}(I) = \frac{1}{2} V^2 , \quad (\text{S-43})$$

which is as such a constant trivial factor that plays a spectating role in the calculation of $F_I(\lambda)$ for single QDs (noninteracting RLM and interacting AIM) in linear response. We note that in the naive calculation in which the finite bandwidth is neglected is UV divergent.

B. Beyond linear response but noninteracting

We now consider the full nonequilibrium transport problem at finite voltage bias. In the presence of strong electron interactions, however, this is largely still a hard open problem. Therefore in this section we restrict ourselves to the simpler case of non-interacting models, where a Landauer-Büttiker type approach holds.¹³ This greatly simplifies the formulation. We note however that although the current calculation is straightforward, the full nonequilibrium noise spectrum is more subtle. In particular, we emphasize that it is crucial to consider a realistic (microscopic) model for the QD circuit since nonuniversal high-energy scales like the hybridization and the conduction electron bandwidth play a role. One must therefore consider from the outset a model with a finite conduction electron bandwidth – the commonly-used wide-band limit will not suffice, as shown below. As such, and for concreteness, in the following we take the metallic free lead density of states to be flat within a band of half-width D , such that $\rho_0(\omega) = \rho_0 \Theta(D - |\omega|)$ and $\rho_0 = 1/2D$. In practice we set $D = 1$.

For non-interacting impurity-type models, the quantum transport problem is controlled by the transmission function $\mathcal{T}(\omega)$, which is independent of both temperature and bias voltage.^{5,13} In general, we can write $\mathcal{T}(\omega) = 4\Gamma_s \Gamma_d \sum_\sigma |G_{sd;\sigma}(\omega)|^2$ where $\Gamma_\alpha = \pi \rho_0 V_\alpha^2$ is the hybridization of the nanostructure frontier orbital $d_{r_\alpha;\sigma}$ to lead $\alpha = s, d$ and $G_{sd;\sigma}(\omega) = \langle\langle d_{r_s;\sigma}; d_{r_d;\sigma}^\dagger \rangle\rangle$ is the full lead-coupled retarded nanostructure Green's function connecting source and drain leads. For clarity, we restore units of e and \hbar in the following.

Taking care to keep track of the finite bandwidth, we now express the current in Landauer-Büttiker form,¹³

$$\langle\hat{I}\rangle = \frac{e}{\hbar} \int d\omega \mathcal{T}(\omega) \times [f_s(\omega) - f_d(\omega)] , \quad (\text{S-44})$$

where $f_\alpha(\omega) = f_{\text{eq}}(\omega - \mu_\alpha)\Theta(D - |\omega - \mu_\alpha|)$ in terms of the chemical potential μ_α for lead α , and we are keeping track of the finite bandwidth with the step function. The bias voltage is $eV_b = \mu_s - \mu_d$, which one can assume is split equally across source and drain leads.

Generalizing the results of Lesovik,¹⁴ we can similarly formulate the nonequilibrium noise spectrum,

$$S(\omega) = \frac{e^2}{\hbar^2} \int d\omega' \left[f_s(\omega' + \omega)\bar{f}_s(\omega')\mathcal{T}(\omega')\mathcal{T}(\omega' + \omega) + f_d(\omega' + \omega)\bar{f}_d(\omega')\mathcal{T}(\omega')\mathcal{T}(\omega' + \omega) \right. \\ \left. + f_s(\omega' + \omega)\bar{f}_d(\omega')(1 - \mathcal{T}(\omega'))\mathcal{T}(\omega' + \omega) + f_d(\omega' + \omega)\bar{f}_s(\omega')\mathcal{T}(\omega')(1 - \mathcal{T}(\omega' + \omega)) \right], \quad (\text{S-45})$$

where we have defined $\bar{f}_\alpha(\omega) = [1 - f_{\text{eq}}(\omega - \mu_\alpha)]\Theta(D - |\omega - \mu_\alpha|)$ for notational simplicity.

The current variance can be obtained by integrating the noise spectrum as before, but now we use the nonequilibrium formula for noninteracting fermions. After some manipulation we obtain,

$$\text{Var}(I) \equiv \langle \hat{I}^2 \rangle - \langle \hat{I} \rangle^2 = \int d\omega S(\omega) \\ = D\Delta_{V_b} + \langle \hat{I} \rangle \delta_{V_b} - \langle \hat{I} \rangle^2, \quad (\text{S-46})$$

where D is the lead bandwidth as before, $\Delta_{V_b} = \frac{e^2}{\hbar^2} \int d\omega \mathcal{T}(\omega)\Theta(D - |\omega - \mu_s|)$ is an effective hybridization, and $\delta_{V_b} = \frac{e}{\hbar} \int d\omega \mathcal{T}(\omega)[\Theta(D - |\omega - \mu_s|) - \Theta(D - |\omega - \mu_d|)]$ describes particle-hole asymmetry in the transmission function at the band edges in a window of width V_b . For a symmetric transmission function $\mathcal{T}(\omega) = \mathcal{T}(-\omega)$ this factor vanishes, $\delta_{V_b} = 0$. The current $\langle \hat{I} \rangle$ is given by Eq. S-44 as usual.

1. Single QD case

Here we consider the single QD case of the RLM (with spin). For simplicity we assume equal coupling to source and drain leads, $V_s = V_d \equiv V$ such that $\Gamma_s = \Gamma_d \equiv \Gamma = \pi\rho_0 V^2$. Then the transmission function reads,

$$\mathcal{T}(\omega) = 8\Gamma^2 |G_{QD}(\omega)|^2 \equiv 4\pi\Gamma A_{QD}(\omega) = \frac{2\Theta(D - |\omega|)}{1 + (\omega - \epsilon_d)^2/4\Gamma^2}, \quad (\text{S-47})$$

where we have used the exact form of the RLM Green's function in Eq. S-27 and approximate $\mathcal{G}_{\text{lead}}(\omega) = -i\pi\rho_0(\omega)$. We take care of the finite lead bandwidth, but neglect the small Lamb shift coming from the real part of the lead Green's function.

S-IV. INTEGRATED CURRENT MEASUREMENTS

In the previous section we considered instantaneous current measurements. However, the formalism can be straightforwardly extended to *integrated* current measurements.¹⁵

We denote the charge collected in the drain lead over some time interval Δt as $C(\Delta t)$. For some time-dependent current trace $I(t)$ we define $C(\Delta t) = \int_0^{\Delta t} dt I(t)$. In the steady state, and taking Δt large, the integrated current becomes $C \simeq \Delta t \langle \hat{I} \rangle$ while the variance of the integrated current is $\text{Var}(C) \simeq \langle (\Delta t \delta \hat{I})^2 \rangle$. Since more information is gained about the parameter of interest from the collected charge the longer we wait, the relevant quantity is really the precision *rate* (or time average) which we denote $\bar{F}_I[\lambda]$. Thus we define,¹⁵

$$\bar{F}_I[\lambda] = \frac{(\partial_\lambda \langle \hat{I} \rangle)^2}{\frac{d}{dt} \text{Var}(C)}. \quad (\text{S-48})$$

It can be shown that $\frac{d}{dt} \text{Var}(C)$ can also be obtained by integrating the current autocorrelation function $S(t)$, or equivalently in terms of the zero-frequency value of the noise spectrum,

$$\frac{d}{dt} \text{Var}(C) = \int dt S(t) = S(\omega = 0). \quad (\text{S-49})$$

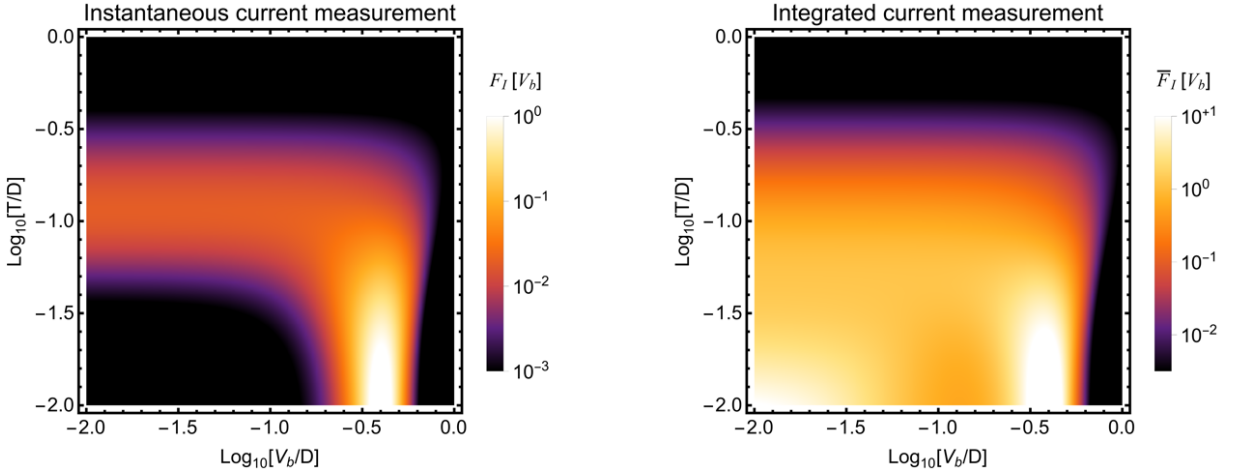


FIG. S-1. Voltmetry precision for estimation of the bias voltage V_b in the non-interacting single-QD resonant level model, as a function of temperature and bias. Left panel shows $F_I[V_b]$ for an instantaneous current measurement, whereas the right panel shows the rate $\bar{F}_I[V_b]$ for an integrated current measurement. Exact results plotted for representative values $\epsilon_d = -0.2$, $\Gamma = 0.05$, and finite lead bandwidth $D = 1$. Recall that the corresponding voltmetric QFI is infinite for this model.

In the interacting but linear-response regime we can take the $\omega \rightarrow 0$ (dc) limit of Eq. S-39 to obtain the completely general relation,

$$S(\omega = 0) = \left(\frac{T}{\pi\hbar} \right) \chi^{dc} \equiv 2T\chi^{dc} h^{-1}. \quad (\text{S-50})$$

Thus we may calculate $\bar{F}_I(\lambda)$ purely from a knowledge of the dc linear response conductance χ^{dc} .

For the noninteracting but nonequilibrium case, we take the $\omega \rightarrow 0$ (dc) limit of Eq. S-45 instead. We obtain,

$$S(\omega = 0) = \frac{e^2}{\hbar^2} \int d\omega' \left[\mathcal{T}(\omega') \left(f_s(\omega') \bar{f}_d(\omega') + f_d(\omega') \bar{f}_s(\omega') \right) - [\mathcal{T}(\omega')]^2 \left(f_s(\omega') - f_d(\omega') \right)^2 \right], \quad (\text{S-51})$$

which is a generalization of the well-known Levitov formula,¹⁴ in which we keep track of the finite lead bandwidth.

A. Voltmetry via current measurements

We briefly compare estimation of the bias voltage using either an instantaneous current measurement $F_I[V_b]$, or an integrated current measurement, $\bar{F}_I[V_b]$. In Fig. S-1 we consider both quantities for the non-interacting RLM in the non-linear regime, as a function of temperature and bias. There are qualitative similarities between the two measures, but the major difference is that the instantaneous current measurement precision has vanishing sensitivity at low T and V_b when the transmission function is small at low energies (as with these parameters); while the integrated current precision rate is relatively enhanced in this region.

B. Magnetometry via current measurements

In Fig. S-2 we present numerical results for the precision for estimation of a magnetic field applied to the QD. The left panel shows the precision for an instantaneous current measurement $F_I(B)$, while in the right panel we show the precision rate $\bar{F}_I(B)$ for an integrated current measurement. This is computed for the interacting AIM, since the field couples to the QD spin, and the non-interacting RLM has no spin dynamics. Therefore we use NRG to compute the linear response conductance, from which the precision is obtained. We are thereby restricted to linear response in the bias voltage and current; the precision is proportional to V_b^2 . We plot universal results in the Kondo regime. Fig. S-2 shows nontrivial behaviour for both, plotted here as a function of rescaled temperature T/T_K and field strength B/T_K , with peak sensitivity in both cases at low T around $B \sim T_K$.

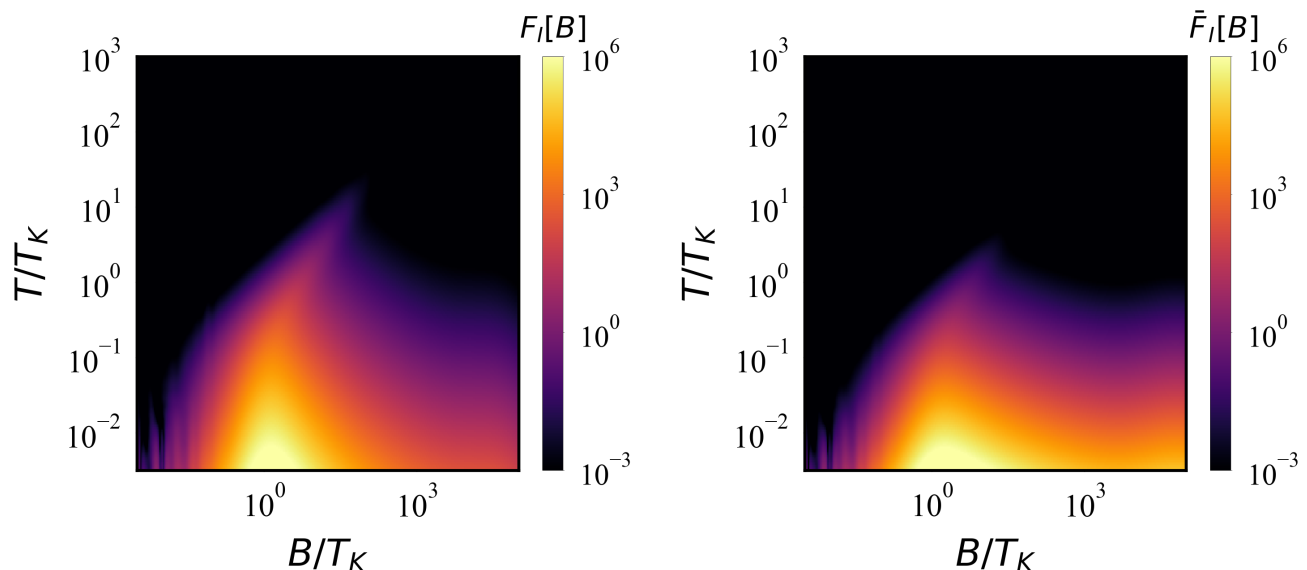


FIG. S-2. Magnetometry precision for estimation of an applied magnetic field B using a current measurement in linear response, for the *interacting* Anderson impurity model. Exact results obtained using NRG, plotted as a function of temperature and field strength, rescaled in terms of the Kondo temperature T_K . Left panel shows $F_I[B]$ for an instantaneous current measurement, whereas right panel shows the rate $\dot{F}_I[B]$ for an integrated current measurement. Shown for representative values $\epsilon_d = -0.15$, $U_d = 0.3$, $V = 0.09$, $D = 1$.

S-V. NRG CALCULATIONS

For many-body calculations of the interacting AIM in the thermodynamic limit, we use Wilson's NRG,⁹ with real-frequency dynamical correlation functions obtained using the full-density-matrix method.¹¹ We exploit conserved charge and spin-projection in the iterative block-diagonalization procedure. A logarithmic discretization parameter $\Lambda = 2.5$ was used and $N_s = 3000$ states retained at each NRG step.

S-VI. VALIDITY OF THE ADIABATIC APPROXIMATION

Our general results on the QFI for an adiabatic perturbation (Eq. 1 of the main text) were illustrated with the example of the AIM and RLM (Figs. 2 and 3). Care must be taken in defining the adiabatic process in such cases, especially when taking the thermodynamic limit of system size $L \rightarrow \infty$.

The standard adiabatic approximation requires that the instantaneous spectral decomposition of the time-evolving Hamiltonian does not contain accidental degeneracies. The AIM and RLM do feature degenerate eigenstates, but typically these are symmetry protected and cannot mix. Specifically, we may label eigenstates by conserved total charge Q and total S^z spin projection; the voltage perturbation V_b and QD magnetic field B preserve these symmetries and so adiabatic evolution occurs independently in these block diagonal symmetry subspaces.

The switch-on protocol $\gamma(t)$ for the perturbation $\hat{H}_1(t) = \gamma(t)\hat{A}$ must be *slow* in an adiabatic process. In particular, the ramp time Δt must be long compared with the inverse minimum spectral gap $\hbar/\Delta E$ to satisfy¹⁶ $\sum_{m \neq n} |\hbar \langle m_\gamma | \dot{n}_\gamma \rangle / (E_n^\gamma - E_m^\gamma)| \ll 1$. This condition can be checked by analyzing the spectrum of the instantaneous Hamiltonian H_γ . Thus as the gap closes ($\Delta E \rightarrow 0$) the adiabatic switch-on time diverges ($\Delta t \rightarrow \infty$). For the AIM and RLM, the system becomes *gapless* as $L \rightarrow \infty$. As discussed in Ref. 17, the adiabatic limit exists in gapless systems when the limits $L \rightarrow \infty$ and $\Delta t \rightarrow \infty$ commute – that is, we can take $\Delta t \rightarrow \infty$ first before $L \rightarrow \infty$. Real many-body systems have this property when weak coupling to the environment or relaxation scattering processes cut off incipient infrared divergences of the energy coming from low-energy modes.¹⁷ We therefore expect our results to hold for the AIM and RLM with finite L for a slow ramp of finite duration. For the noninteracting RLM the characteristic spectral gap is $\Delta E \sim D/L$ due to the single-particle states, whereas for the interacting AIM we have $\Delta E \sim D/(4^L)$ due to strong correlation effects. In the thermodynamic limit $L \rightarrow \infty$ where both RLM and AIM are gapless, the adiabatic switch-on of the perturbation in principle therefore requires an infinite ramp time $\Delta t \rightarrow \infty$.

On a technical level, the calculation of the QFI in the thermodynamic limit is handled automatically using Eq. 1b

and Eq. 6 through the formulation involving integrals over the correlation functions $\chi(\omega)$ or $\bar{K}(\omega)$, which simply become continuous functions of ω within a finite bandwidth D as $L \rightarrow \infty$. For finite L note that $\chi(\omega)$ and $\bar{K}(\omega)$ consist of a discrete sum of poles, obtainable from their Lehmann representation. This is used in Fig. 2 and 3 for the finite-size scaling analysis. Controlled finite-size approximations that converge to the thermodynamic limit can be naturally achieved by broadening the discrete poles by e.g. convolution of the spectra with a Gaussian kernel.

In the second part of the paper we consider instead the metrological precision for a current measurement in nanoelectronics devices in the thermodynamic limit $L \rightarrow \infty$, rather than the QFI for the optimal many-body measurement. Here we employ the standard assumption that the voltage bias V_b is switched on adiabatically in the distant past (but the parameter λ can be a parameter of \hat{H}_0 , \hat{H}_1 or even T). The adiabatic approximation has a long history in the quantum transport context.^{4,18} In experiment, where the nanostructure is contacted with a macroscopic external electronic circuit, the voltage bias is obviously switched on in a finite time, yet the measured linear-response transport coefficients are accurately given by the predictions of the Kubo formula which relies on the linear response assumption.^{4,6,19} Indeed, detailed universal scaling predictions using the Kubo formula for the electrical conductance in strongly correlated critical systems have been quantitatively confirmed experimentally.^{20–22} We conclude that the adiabatic switch-on of the voltage bias in nanoelectronics systems in the thermodynamic limit is entirely practical.

S-VII. SUPER-HEISENBERG SCALING OF THE QFI

Fig. 2 of the main text shows a scaling analysis of the QFI for the adiabatic bias perturbation V_b with increasing system size L in the noninteracting RLM and the interacting AIM. Here L refers to the number of fermionic sites in each of the 1d nanowire leads. The total number of fermionic degrees of freedom is thus $2L + 1$ in both cases, including the QD. For the RLM, the model is quadratic in fermion field operators and so the Hamiltonian operator can be brought to diagonal form by a canonical transformation. All physical properties can then be expressed in terms of the independent single-particle (one-body) states of the diagonal representation. In particular, any operator of arbitrary M -body complexity can be formulated in this way, and so the optimal global measurement for parameter estimation depends only on these states. The QFI can then be formulated in terms of single-particle states for noninteracting systems. For the RLM, the quantum ‘resource’ is in some sense therefore these single-particle states, of which we have $2L + 1$. Using exact diagonalization in the single-particle sector we are able to go to large system sizes and see a robust scaling $\max(F_Q[V_b]) \sim L^2$. This is Heisenberg scaling,^{23–27} which already shows a quantum advantage over metrology with classical systems. The classical Fisher information (FI) is extensive in classical systems and for uncorrelated quantum states (the FI of a product state is the sum of the FI for its subsystems¹). Quantum correlations are needed to reach the observed quadratic scaling.

For interacting systems such as the AIM (with quartic coupling terms), there is no simple single-particle representation and in general one must construct the Hamiltonian matrix in the full many-particle basis. The full Fock space is of dimension 4^{2L+1} and is exponentially large in the system size. For global perturbations (such as V_b) that imprint strongly on a large fraction of the many-particle states, and with the optimal many-body measurement with support on the global system, we find that the QFI can scale as $\max(F_Q[V_b]) \sim (4^L)^2$, indicating that the quantum ‘resource’ here is in some sense the set of many-particle states, of which we have exponentially many in number. Thus for both RLM and AIM we see a kind of quadratic scaling ($F_Q[V_b] \sim N^2$, where for the RLM $N \equiv L$ for single-particle states, whereas for the AIM $N \equiv 4^L$ for the many-particle states. The subtleties of apparent super-Heisenberg scaling are discussed in Refs. 27 and 28.

We emphasize that a more modest scaling would be expected if: (i) the measurement were confined to a subspace of the full system (for example one or a few local sites); (ii) the measurement was restricted to M -body terms, with $M < 2L + 1$ (but still with support on the full system); (iii) the perturbation is not global and therefore imprints strongly on only a small fraction of the many-body states; (iv) we deal with some specific practical measurement rather than the optimal one.

Regarding point (i), the thermometric QFI for a local measurement on the QD (in a Kondo model variant) was considered in Ref. 29, and was found to remain finite in the thermodynamic limit of an infinite conduction electron bath. Point (iii) is addressed specifically in Fig. 3 where we consider a local perturbation $B\hat{S}_d^z$ to the QD. Even the optimal global, many-body measurement on the full system here yields a QFI $F_Q[B]$ that remains finite even as $L \rightarrow \infty$. We illustrate point (iv) in Fig. 4 where we consider a current measurement. Even though the current is a global object and we take the thermodynamic limit $L \rightarrow \infty$, the precision $F_I[V_b]$ and $F_I[B]$ are finite.

Finally, we touch upon the time resources required to do parameter estimation for an adiabatic perturbation.²⁷ As discussed above in Sec. S-VI, the adiabatic switch-on protocol involves a ramp time that diverges as the system size increases. The results for the adiabatic QFI for large L are therefore to be understood as a fundamental bound rather than a guide for experiments, since in this limit meaningful measurement statistics cannot be gathered in practice. For finite L (and hence a finite preparation time Δt) this has implications for the effective QFI scaling, since the effective

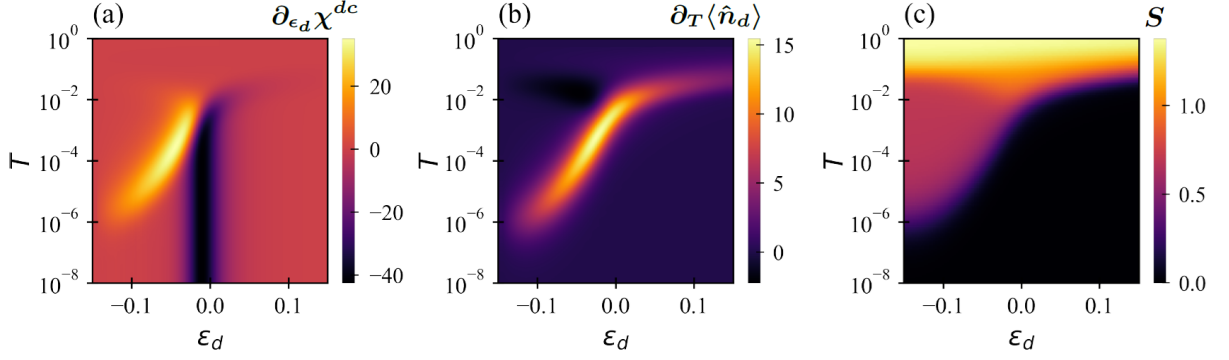


FIG. S-3. Precision of thermodynamic entropy estimation from current measurements in QD systems modelled by the AIM in the Kondo regime. (a) Derivative of the experimentally-measurable linear-response electrical conductance χ^{dc} with respect to the QD potential ϵ_d as a function of T and ϵ_d . (b) Temperature derivative of the experimentally-measurable QD charge $\langle \hat{n}_d \rangle$ as a function of T and ϵ_d . (c) Thermodynamic entropy S of the QD as a function of T and ϵ_d . Shown for representative values of AIM model parameters $U_d = 0.3$, $V = 0.09$ ($\Gamma = 0.013$) and $B = 0$ with a flat conduction electron band of half-width $D = 1$.

QFI scales linearly in the number of independent measurements N . In a given amount of experimental measurement time τ , we can perform $\tau/\Delta t$ independent measurements. But for adiabatic evolution Δt itself increases with system size as the excitation gaps close. The precision is lower bounded by a quantity which scales as $(\tau 4^L)^{-1}$ for the AIM or $(\tau L)^{-1}$ for the RLM. This should be analyzed on a case-by-case basis.

The above discussion highlights the limitations of interpreting the QFI for global measurements in many-body systems. However, the QFI does provide a benchmark against which feasible experimental measurements (such as the current) should be compared. Our ultimate conclusion is that practical measurements that leverage many-body effects and have support on the full system may be vastly superior to local or few-body measurements. This provides ample motivation for designing nonstandard measurement protocols for advanced quantum sensing applications.

S-VIII. ENTROPY ESTIMATION

In Fig. 4d of the main text we provide a non-standard application of the parameter estimation paradigm, to thermodynamic quantities. We focus on the thermodynamic entropy of the QD in the AIM, defined $S = S_{\text{tot}} - S_0$ where $S_{\text{tot}} = -\partial_T \mathcal{F}$ is the equilibrium entropy of the full lead-coupled QD system \hat{H}_0 , and S_0 is the entropy of a trivial reference state in which the QD is unoccupied (in practice obtained for $\epsilon_d \rightarrow \infty$). Here $\mathcal{F} = -T \ln(Z_0)$ is the free energy of the system (Z_0 is the partition function of \hat{H}_0 as before). Recently,³⁰ it was pointed out that since $\partial_T \partial_{\epsilon_d} \mathcal{F} = \partial_{\epsilon_d} \partial_T \mathcal{F}$, one can write down a local Maxwell relation,

$$S(\epsilon_d, T) = - \int_{\epsilon_d}^{\infty} d\bar{\epsilon} \partial_T \langle \hat{n}_d \rangle_{\bar{\epsilon}, T}, \quad (\text{S-52})$$

for the entropy S in terms of the experimentally measurable QD charge $\langle \hat{n}_d \rangle = \partial_{\epsilon_d} \mathcal{F}$, where $\hat{n}_d = \sum_{\sigma} d_{\sigma}^{\dagger} d_{\sigma}$. Indeed, the entropy of a single QD modelled by the AIM in the strongly correlated regime was extracted experimentally in Ref. 30 in this way.

Here we consider the precision of estimation of S from a current measurement, $F_I[S] = |\partial_S \langle \hat{I} \rangle|^2 / \text{Var}(I)$, as defined from Eq. 9 of the main text. We wish to express the precision in terms of the experimentally-measurable quantities $\langle \hat{n}_d \rangle$ and $\chi^{dc} = \partial_{V_b} \langle \hat{I} \rangle$. We do this by writing $\partial_S \langle \hat{I} \rangle = \partial_{\epsilon_d} \langle \hat{I} \rangle / \partial_{\epsilon_d} S$ and then exploiting the Maxwell relation $\partial_{\epsilon_d} S = -\partial_T \langle \hat{n}_d \rangle$ as used above. This leads to,

$$F_I[S] = \frac{|\partial_{\epsilon_d} \langle \hat{I} \rangle / \partial_T \langle \hat{n}_d \rangle|^2}{\text{Var}(I)}. \quad (\text{S-53})$$

For the AIM, we compute both $\langle \hat{I} \rangle$ and $\langle \hat{n}_d \rangle$ as a full function of ϵ_d and T using NRG. From these we easily obtain their numerical derivatives, which are plotted in Figs. S-3(a,b). For reference, we show the entropy S itself in panel (c). Evaluation of Eq. S-53 using the data in Figs. S-3(a,b) yields the plot in Fig. 4d of the main text.

We note that the entropy in Fig. S-3(c) shows characteristic regions corresponding to the renormalization group fixed points of the AIM.⁸ In particular we have $S = \ln(4)$ at high temperatures for the free-orbital fixed point corresponding

to quasi-degenerate empty, singly-occupied, and doubly-occupied QD states. We also see a local-moment regime of degenerate QD spin states giving $S = \ln(2)$ (but charge degrees of freedom frozen out), and $S = 0$ fermi liquid regimes. For $\epsilon_d < 0$ and $T \ll T_K$ the quenched entropy has a nontrivial origin in the Kondo effect.⁸ Note that the metallic AIM does not support any critical points; the complex behavior of Fig. S-3(c) arises from crossovers, rather than transitions, between fixed points. The precision diagram Fig. 4d can now be understood: we see enhanced sensitivity to estimation of the entropy using a current measurement when the entropy itself changes rapidly with ϵ_d and T . This occurs along the crossovers between the renormalization group fixed points described above.

-
- ¹ G. Tóth and I. Apellaniz, J. Phys. A: Math. Theor **47**, 424006 (2014).
² P. Hauke, M. Heyl, L. Tagliacozzo, and P. Zoller, Nat. Phys. **12**, 778 (2016).
³ D. N. Zubarev, Soviet Physics Uspekhi **3**, 320 (1960).
⁴ R. Kubo, J. Phys. Soc. Jpn. **12**, 570 (1957).
⁵ E. Minarelli, J. Rigo, and A. Mitchell, (2022), arXiv:2209.01208.
⁶ M. Pustilnik and L. Glazman, J. Phys. Condens. Matter **16**, R513 (2004).
⁷ U. Meirav, M. A. Kastner, and S. J. Wind, Phys. Rev. Lett. **65**, 771 (1990).
⁸ A. Hewson, *The Kondo problem to heavy fermions* (Cambridge Studies in Magnetism, CUP, 1993).
⁹ R. Bulla, T. A. Costi, and T. Pruschke, Rev. Mod. Phys. **80**, 395 (2008).
¹⁰ Y. Meir and N. S. Wingreen, Phys. Rev. Lett. **68**, 2512 (1992).
¹¹ A. Weichselbaum and J. von Delft, Phys. Rev. Lett. **99**, 076402 (2007).
¹² D. Ding, Z. Liu, B. Shi, G. Guo, K. Mølmer, and C. Adams, Nat. Phys. **18**, 1447 (2022).
¹³ M. Büttiker, Y. Imry, R. Landauer, and S. Pinhas, Phys. Rev. B **31**, 6207 (1985).
¹⁴ G. B. Lesovik, JETP Letters **49**, 513 (1989).
¹⁵ “We thank Mark Mitchison for this suggestion and for helpful discussions.”.
¹⁶ D. Comparat, Phys. Rev. A **80**, 012106 (2009).
¹⁷ A. Polkovnikov and V. Gritsev, Nat. Phys. **4**, 477 (2008).
¹⁸ J. Henheik and S. Teufel, Rev. Math. Phys. **33**, 2060004 (2021).
¹⁹ D. Goldhaber-Gordon, H. Shtrikman, D. Mahalu, D. Abusch-Magder, U. Meirav, and M. A. Kastner, Nature **391**, 156 (1998); W. Van der Wiel, S. D. Franceschi, T. Fujisawa, J. Elzerman, S. Tarucha, and L. Kouwenhoven, Science **289**, 2105 (2000).
²⁰ Z. Iftikhar, A. Anthore, A. K. Mitchell, F. D. Parmentier, U. Gennser, A. Ouerghi, A. Cavanna, C. Mora, P. Simon, and F. Pierre, Science **360**, 1315 (2018).
²¹ A. K. Mitchell, L. A. Landau, L. Fritz, and E. Sela, Phys. Rev. Lett. **116**, 157202 (2016).
²² W. Pouse, L. Peeters, C. L. Hsueh, U. Gennser, A. Cavanna, M. A. Kastner, A. K. Mitchell, and D. Goldhaber-Gordon, Nat. Phys. **19**, 492 (2023); D. B. Karki, E. Boulat, W. Pouse, D. Goldhaber-Gordon, A. K. Mitchell, and C. Mora, Phys. Rev. Lett. **130**, 146201 (2023).
²³ K. Gietka, F. Metz, T. Keller, and J. Li, Quantum **5**, 489 (2021).
²⁴ R. Demkowicz-Dobrzański, J. Kołodyński, and M. Guţă, Nat. Commun. **3**, 1063 (2012).
²⁵ M. Zwierz, C. A. Pérez-Delgado, and P. Kok, Phys. Rev. A **85**, 042112 (2012).
²⁶ M. Zwierz, C. A. Pérez-Delgado, and P. Kok, Phys. Rev. Lett. **105**, 180402 (2010).
²⁷ M. M. Rams, P. Sierant, O. Dutta, P. Horodecki, and J. Zakrzewski, Phys. Rev. X **8**, 021022 (2018).
²⁸ J. Yang, S. Pang, A. del Campo, and A. N. Jordan, Phys. Rev. Res. **4**, 013133 (2022).
²⁹ G. Mihailescu, S. Campbell, and A. K. Mitchell, Phys. Rev. A **107**, 042614 (2023).
³⁰ T. Child, O. Sheekey, S. Lüscher, S. Fallahi, G. C. Gardner, M. Manfra, A. K. Mitchell, E. Sela, Y. Kleeorin, Y. Meir, and J. Folk, Phys. Rev. Lett. **129**, 227702 (2022).